

**DEVELOPMENT OF THE HYBRID STORAGE
SYSTEM USING THERMOELECTRIC
GENERATOR**

ONG WEI CHAO

UNIVERSITI TUNKU ABDUL RAHMAN

**DEVELOPMENT OF THE HYBRID STORAGE SYSTEM USING
THERMOELECTRIC GENERATOR**

ONG WEI CHAO

**A project report submitted in partial fulfilment of the
requirements for the award of Bachelor of Engineering
(Honours) Mechanical Engineering**

**Lee Kong Chian Faculty of Engineering and Science
Universiti Tunku Abdul Rahman**

May 2022

DECLARATION

I hereby declare that this project report is based on my original work except for citations and quotations which have been duly acknowledged. I also declare that it has not been previously and concurrently submitted for any other degree or award at UTAR or other institutions.

Signature :



Name : ONG WEI CHAO

ID No. : 991201-01-6501

Date : 16 MAY 2022

APPROVAL FOR SUBMISSION

I certify that this project report entitled “**DEVELOPMENT OF THE HYBRID STORAGE SYSTEM USING THERMOELECTRIC GENERATOR**” was prepared by **ONG WEI CHAO** has met the required standard for submission in partial fulfilment of the requirements for the award of Bachelor of Engineering (Honours) Mechanical Engineering at Universiti Tunku Abdul Rahman.

Approved by,

Signature : *Bernard saw*

Supervisor : Ir Ts Dr Bernard Saw Lip Huat

Date : 16 MAY 2022

The copyright of this report belongs to the author under the terms of the copyright Act 1987 as qualified by Intellectual Property Policy of Universiti Tunku Abdul Rahman. Due acknowledgement shall always be made of the use of any material contained in, or derived from, this report.

© 2022, Ong Wei Chao. All right reserved.

ACKNOWLEDGEMENTS

I would like to thank everyone who had contributed to the successful completion of this project. I would like to express my gratitude to my research supervisor, Dr. Bernard Saw Lip Huat for his invaluable advice, guidance and his enormous patience throughout the development of the research.

In addition, I would also like to express my gratitude to my loving parents and friends who had helped and given me encouragement throughout the project.

Without the supports from them, the project would not be accomplished easily. All of the helps and supports received are truly appreciated from the bottom of my heart.

ABSTRACT

Thermoelectric module (TEM) is a solid-state semiconductor with n-type and p-type materials interconnected by metal strips. The module is only a small thin flat plate with no moving parts, but it can convert the electrical energy into thermal energy and vice versa. It can be used as a heat pump under Peltier effect or an electric generator under Seebeck effect. In this study, the thermoelectric module will be used as a heat pump, where it requires current input to create a cold side and a hot side on its surface to transfer the heat from one side to the other. There is no available hybrid storage system in the market that supports both heating and cooling effects. Therefore, this study will provide an insight on the application of simultaneous cooling and heating chambers by TEM. A CFD simulation model is performed by using ANSYS software to investigate the performance of TEM under heat load condition. Then, two insulation chambers are built to analyze the performance of TEM when it is used for cooling or heating purpose. Three operation modes are studied in this paper, which are cooling mode, heating mode and simultaneous cooling and heating mode. Under cooling mode, the air temperature inside the chamber able to reach 5.89 °C within 30 minutes, meanwhile the chamber reaches 61.66 °C within 25 minutes under heating mode. On the other side, the cooling chamber reaches 9.66 °C and the heating chamber reaches 39.09 °C for the simultaneous mode, the two chambers achieve equilibrium state within 20 minutes of operation. The experimental COP of the chamber for cooling mode is 0.05 while the heating mode is 0.12.

TABLE OF CONTENTS

DECLARATION		i
APPROVAL FOR SUBMISSION		ii
ACKNOWLEDGEMENTS		iv
ABSTRACT		v
TABLE OF CONTENTS		vi
LIST OF TABLES		viii
LIST OF FIGURES		ix
LIST OF SYMBOLS / ABBREVIATIONS		xi
LIST OF APPENDICES		xii
CHAPTER		
1	INTRODUCTION	1
1.1	General Introduction	1
1.2	Importance of the Study	3
1.3	Problem Statement	3
1.4	Aim and Objectives	3
1.5	Scope and Limitation of the Study	4
1.6	Contribution of the Study	4
1.7	Outline of the Report	4
2	LITERATURE REVIEW	5
2.1	Introduction	5
2.2	Thermoelectric module	5
2.5	Solar-Thermoelectric system	14
2.6	Self-driven thermoelectric model	17
2.7	Summary	18
3	METHODOLOGY AND WORK PLAN	19
3.1	Introduction	19
3.2	Simulation model	20
3.2.1	Setup of ANSYS software	20

3.3	Experimental design	22
3.3.1	Cooling mode	22
3.3.2	Heating mode	23
3.3.3	Simultaneous cooling and heating mode	24
3.3.4	Apparatus and equipment	25
3.3.5	Preliminary testing on TEC1-12706	31
3.3.6	Circuit diagram	32
3.4	Summary	34
4	RESULTS AND DISCUSSION	35
4.1	Introduction	35
4.2	Simulation model	35
4.3	Cooling mode	38
4.3.1	Cooling load test	41
4.3.2	Comparison with theoretical value	44
4.4	Heating mode	44
4.4.1	Heating test	46
4.4.2	Comparison with theoretical value	48
4.5	Simultaneous cooling and heating mode	49
4.5.1	Theoretical calculation on COP	51
4.6	Summary	52
5	CONCLUSIONS AND RECOMMENDATIONS	54
5.1	Conclusions	54
5.2	Recommendations for future work	55
	REFERENCES	56
	APPENDICES	60

LIST OF TABLES

Table 2.1:	Comparison of different solar-driven TE refrigerator	17
Table 3.1:	Details of ANSYS setup	22
Table 3.2:	Performance of TEC1-12706 under different current	31
Table 4.1:	Grid dependency test with 8 iterations	36
Table 4.2:	Power consumption of equipment under cooling mode	41
Table 4.3:	Power consumption of equipment under heating mode	46
Table 4.4:	Power consumption of equipment under simultaneous cooling and heating mode	50
Table 4.5:	COP of chamber under three different operation modes	53

LIST OF FIGURES

Figure 2.1:	Schematic diagram of a complete thermoelectric circuit (Hermes & Barbosa Jr., 2012)	5
Figure 2.2:	COP of cooling mode versus current for single- and two-stage thermoelectric at different cold side boundary conditions (Nami, Nemati, Yari & Ranjbar, 2017).	12
Figure 3.1:	Flow chart of the project	19
Figure 3.2:	Geometry of insulation chamber in ANSYS with four inlets	20
Figure 3.3:	Chamber design for cooling mode	23
Figure 3.4:	Internal of the chamber with layered aluminium sheet	23
Figure 3.5:	Chamber design for heating mode	24
Figure 3.6:	Schematic drawing of simultaneous mode	24
Figure 3.7:	Chamber designs for simultaneous cooling and heating mode	25
Figure 3.8:	Thermoelectric module with part number TEC1-12706	26
Figure 3.9:	GW Instek GPC-3030 power supply	28
Figure 3.10:	TTi QPX600D power supply	28
Figure 3.11:	Graphtec midi logger GL840	29
Figure 3.12:	Thermocouple type-K	30
Figure 3.13:	Sub-assembly of Peltier module	30
Figure 3.14:	Graph of TEC1-12706 cold side temperature at different current	32
Figure 3.15:	Series connection of two Peltier modules	32
Figure 3.16:	Parallel connection of two Peltier modules	33
Figure 3.17:	Circuit diagram for four individual power outputs	34
Figure 4.1:	Graph of grid dependency test with wall temperature vs mesh elements	36

Figure 4.2:	Finalized grid model with 10 mm body sizing meshing	37
Figure 4.3:	Temperature distribution on the wall of the fluid domain	38
Figure 4.4:	Graph of temperature profile under cooling mode	40
Figure 4.5:	Graph of temperature profile with heat load test under cooling mode	42
Figure 4.6:	Graph of temperature profile under heating mode	45
Figure 4.7:	Graph of temperature profile under simultaneous cooling and heating mode	50

LIST OF SYMBOLS / ABBREVIATIONS

c_p	specific heat capacity, J/(kg·K)
K	Thermal conductivity
α	Seebeck coefficient
ρ	density, kg/m ³
T	Temperature
COP	Coefficient of Performance
TEM	Thermoelectric Module
TEC	Thermoelectric Cooler
TEG	Thermoelectric Generator

LIST OF APPENDICES

Appendix A:	Figures	60
-------------	---------	----

CHAPTER 1

INTRODUCTION

1.1 General Introduction

Refrigerator is one of the most important household appliances in our daily lives. It helps to prolong the shelf life of the fresh foods and groceries by keeping it at low temperature. When the food is stored in a low temperature environment, it will slow down the growth of the bacteria inside the food which might cause it to spoil. As a result, refrigerator could help in the reduction of food wastage issues and enables household to buy the fresh foods in bulk quantity for storage.

On the other hand, food warmer is used to maintain the serving temperature of prepared food. It helps to deliver the dishes for customers at the best tasting temperature and flavour. Food warmer also could re-heat the cooled dishes.

The basic working principle of refrigerator is based on the vapour compression cycle, which comprises of evaporator, compressor, condenser and expansion valve. The refrigerant is used to transfer the heat out from the conditioned environment to the heat sink such as air, by flowing through the components mentioned above and undergo phase changes, the heat is transferred between the two mediums under the law of thermodynamics. Due to these essential components required to build a refrigerator, it is always large in size and it is not designed for portable use. However, there are a few designs of portable fridge which are popular in the recent years and most of them also operate based on the idea of refrigeration cycle. The complete vapour compression cycle is built on a smaller scale so that it is able to squeeze inside a small container. In contrast, this type of appliance is always higher in cost and pricey due to the high performance and advanced technology of the product.

In the recent studies, thermoelectric have been integrated into different type of applications, including electric generation, refrigeration, electronic cooling, vaccine storage and biomedical devices. Its characteristic of reversible energy conversion had made it to be widely used in the industry.

As the environmental issues arise with the advance development of technology nowadays, thermoelectric starts to become a substitute and emerging technology for various applications.

In this context, thermoelectric is considered to be a substitute for the conventional refrigeration cycle in cooling system. Thermoelectric module (TEM) is a solid-state semiconductor with n-type and p-type materials interconnected by metal strips, the module is only a thin flat plate and no moving parts. However, it is able to directly converts the electrical energy into the thermal energy and vice versa with one single thin plate. Thermoelectric modules are mechanically simple and free of noise, it can simply transfer the thermal energy from one side to the other without any mechanical equipment due to the Peltier effect (Cai et. al., 2019). Besides, the thermoelectric has very fast response time and also small in size, which make it suitable to be implemented on the portable cooler devices. Moreover, both of the heating and cooling effect can be achieved by TEM, changing the polarity of the input power will make the direction of heat transfer to be reversed. It also provides a good control of temperature, either to cool down or heat up an enclosure very quickly.

Thermoelectric devices can be classified into two, which are thermoelectric cooler (TEC) and thermoelectric generator (TEG). TEC use the electricity to transfer the heat between two surfaces through the Peltier effect; TEG able to convert the heat flux into electrical energy through the Seebeck effect. In the recent studies, multi-stage thermoelectric systems have been developed to further increase the efficiency and performance of thermoelectric (Belovski & Aleksandro, 2019). Some researchers also utilized the electricity generated from TEG to power up the TEC system, which is also known as combined self-driven TEG-TEC system. Different types of electrical circuit configuration of this combined system had been developed and studied to enhance the coefficient of performance (COP) of cooling effect.

In this study, an experimental prototype consists of Peltier modules will be tested for its performance of heating and cooling mode. The target cooling temperature is 5 °C. A simulation model will be generated to prove the design concept and the working of the thermoelectric module.

1.2 Importance of the Study

The result of this present study may develop a new design of portable hybrid storage device which able to cool down or heat up the temperature of a small enclosure space. This study also offers an alternative design for the existing portable mini fridge in the market. The working principle of thermoelectric is different from the conventional refrigeration cycle in which it does not require any refrigerant that is harmful to the environment. This study able to provide a solution for the portable fridge with no harmful gases to the environmental. Besides, this study may offer a lower cost and efficient refrigerator with simple electronic devices, which include of the thermoelectric modules. Furthermore, this study may provide an insight to increase the COP of thermoelectric based system.

1.3 Problem Statement

The application of thermoelectric in portable storage system is still lack of developments due to its lower efficiency. It is mainly used to harvest the heat energy from a system to utilize the waste energy for other operation. Although the performance of different configurations of the thermoelectric modules have been studied, its application on the portable hybrid storage system is yet to be explored and researched. Currently there are few designs of miniature fridge for medical application, but it is not commercialized in the market. It is desirable to achieve the cooling and heating effect on a single storage device as it is new in the market.

1.4 Aim and Objectives

The main aim of this study is to develop a hybrid storage system by using the thermoelectric generator. This study also investigates the coefficient of performance (COP) of the thermoelectric modules. The objectives of this study were:

1. To design the hybrid cooler and warmer storage using thermoelectric generator.
2. To construct the hybrid cooler and warmer storage system.
3. To analyse the performance of the hybrid storage system using computational fluid dynamic.

1.5 Scope and Limitation of the Study

This study will be focused on the design of thermoelectric system for heating and cooling purpose. The target cooling temperature is set to be 5 °C which is comparable to the household refrigerator. Besides, the efficiency and COP of the storage system will be evaluated under actual working environment. The attainable COP of the cooling mode should be around 0.2 – 0.5, which is limited to the performance of the thermoelectric module.

1.6 Contribution of the Study

The performance of thermoelectric module under heating and cooling condition will be discussed in this report. This study can provide an insight on the application of thermoelectric module in the market, especially the simultaneous cooling and heating chambers. This study also outlines the COP of the TEM, which is the main concern for refrigeration or heat pump cycle as it evaluates the effectiveness of the system.

1.7 Outline of the Report

This report will discuss the performance of hybrid storage system with thermoelectric modules. Chapter 1 provides an overview of the project, the main objectives, scope and limitation of this project. Chapter 2 is a study on the literature review to investigate the previous work done by the researchers. This chapter also looks into the latest technology used to design the thermoelectric system. Chapter 3 describes the methodology and work plan of the project. The simulation model and prototyping process will be discussed in detailed. The results obtained from the experiment of prototype will be presented in Chapter 4. This chapter also highlights key findings, reasonings and justification on the project result. Lastly, Chapter 5 concludes the findings in this project and some recommendations for future works.

CHAPTER 2

LITERATURE REVIEW

2.1 Introduction

The development of the thermoelectric module had attained a great interest for the researchers since mid-1900s due to its numerous of advantages in industry application, such as small in size, compact, direct conversion of energy and reliability. This section will review the different configurations of the thermoelectric system in the way of electrically and mechanically. In addition, the thermoelectric system modelling approaches will be reviewed as well.

2.2 Thermoelectric module

Thermoelectric is a solid-state module that uses the electrical energy to create a temperature difference across a pair of two dissimilar materials. For instance, an array of p-type and n-type blocks of semiconductor is sandwiched between two ceramic wafers as shown in Figure 2.1. When the electrons move from p- to n-type through conductor, the electrons will absorb the energy from the surrounding to jump into a higher energy state, thus creating a cold side (Hermes & Barbosa Jr., 2012). On the other hand, the electrons will release the energy to the surrounding (hot side) when it moves from n- to p-type side.

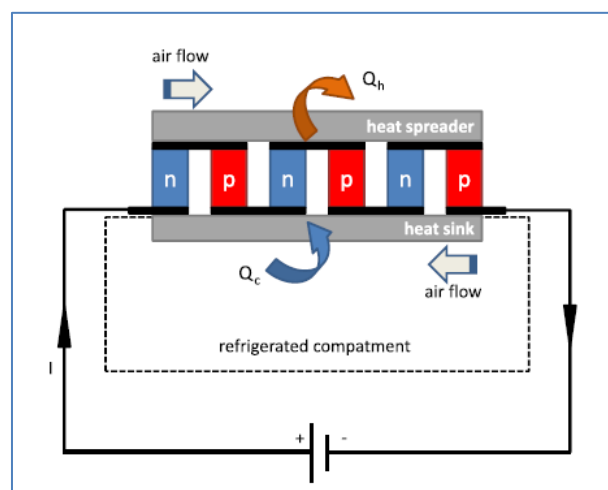


Figure 2.1: Schematic diagram of a complete thermoelectric circuit (Hermes & Barbosa Jr., 2012)

The performance of a thermoelectric material can be determined by a dimensionless parameter, which is known as figure of merit (ZT).

$$ZT = \frac{\alpha^2}{k} \sigma T$$

where α is Seebeck coefficient, σ is electrical conductivity, k is thermal conductivity and T is temperature. To achieve a higher performance of the thermoelectric modules, the conducting material must be low thermal conductivity and high electrical properties (He et. al. , 2015). For example, a typical material being used is Bismuth Telluride (Bi-Te) with ZT value of 2.4 at room temperature. However, the cooling capacity and performance of the thermoelectric material is still insufficient to be competitive with the conventional refrigerator. This is because the COP of a thermoelectric device is typically low for about 0.5, whereas comparing to the refrigerator of about 2.5 (Shafee, Gnanasekaran and Samuel, 2018). Therefore, different models of thermoelectric devices had been developed and studied to improve the COP.

According to Zhao and Tan (2014), the length of thermoelement is the most dependent factor that affect the COP and cooling capacity of the TEM. The COP will be increased with the length, while the cooling capacity inversely proportional to the length of thermoelement. However, the properties of the TEM are defined by manufacturer, hence the improvement of the module can be made by the design of cooling system. The authors had mentioned that the air-cooled heat sink can result in higher cooling COP as compared to the heat pipe. Heat pipe is not efficient for the TEM as the thermal transfer rate is lower.

Meng, Wang and Zhang (2013) had developed a transient TE model which based on the temperature-dependent properties of the TE materials. Fourier's thermal conductivity effect was minimized at a low temperature difference and low operating current thus maintain the cold side at a high cooling capacity. Meanwhile, the cold side temperature was increasing with high current applied due to the Fourier's effect was dominating over the Peltier's effect. Therefore, the TE module was unable to perform the cooling effect at the cold side, leading to a significantly low COP and low cooling capacity. Besides, the temperature difference between the hot and cold side

also decreased with higher cooling load, hence maintaining the high cooling capacity.

2.3 Thermoelectric Cooling and Heating System

Jugsujinda, Vora-ud and Seetawan (2011) had analyzed the performance of a thermoelectric cooler used in a refrigerator container with 25 x 25 x 35 cm³. One module of TEC1-12075 was used in the experiment. The cold side temperature of the TEC was decreased from 30 °C to -4.2 °C within the first hour of operation, whereas the temperature inside the refrigerator reduced from 30 °C to 20 °C only. The performance of the refrigerator was not efficient as there was only one module for such a big container, moreover there was no fan at the cold side of the module. However, it proved the concept of utilizing the TEC as a cooling device was functionable, the maximum COP achieved was 3.0 for the module and 0.65 for the cooling space.

A simultaneously thermoelectric cooling and heating unit prototype was developed by Yilmazoglu (2015) to study the COP of the thermoelectric module. In the design, a single-stage TEM was placed in between two antisymmetric ducts with fans. The result showed that the COP of heating effect was ranging from 2.5-5.0 at different fan speeds, with the maximum increment of air temperature by 11.0 °C. On the other hand, the COP of the cooling was relatively smaller with the value of 0.4-1.0, maximum decrement of temperature by 1.2 °C only. It can be concluded that the heating performance is excellent by the TEM and it is ideal to be implemented for the air heater during the cold days. However, the performance of the cooling effect is not sufficient to be implemented in the HVAC system. The study also highlighted that the COP of the system is increased when the mass flow rate of the air is increased. Therefore, when the TEM is placed in an enclosure or container, a small fan should be installed to induce the forced convection at both cooling and heating chamber. This might help to enhance the efficiency of the TEM and achieve the steady state faster.

A simulation model of air heater operated by thermoelectric modules was established by Meng et. al. (2015) to investigate the optimal performance of the system. The COP of the system increased with the voltage and achieved

optimal COP at the input power of around 4 – 6 V, then it dropped with higher voltage. The optimal value of COP was about 2.4 – 2.8. Besides, it was found that the COP decreased when the temperature difference between the hot side and the chamber air increased. It was not an ideal case as the system will require higher input power in order to heat up the chamber air. Furthermore, thermal resistance of the heat pipes that attached to the TEM also contribute to the performance of the system, as the lower thermal resistance can reduce the heat loss from the system and achieve a higher COP.

Ibañez-Puy et. al. (2017) analyzed the performance of a thermoelectric heating-cooling prototype to be used for the building applications. The maximum COP obtained was around 0.75 for the cooling effect while 1.40 for the heating effect. It can be seen that the COP for the heating effect is always higher than the cooling, this is due to the Joule heating effect where it is always negatively impact on the cold side. Besides, this study had provided the important insight that using more TEMs operate at lower voltage range is better than fewer TEMs operates at high voltage range. This would help to reduce the Joule heating effect and the COP could be further enhanced, especially at the cooling side.

Afshari (2020) also compared the COP value in both heating and cooling mode of a water-cooled TE refrigerator prototype. It can be clearly seen that the heating mode COP was 233 % higher than cooling mode. As a result, the cooling mode will have higher power consumption due to its low energy efficiency. The author also highlighted that the imported and extracted thermal energy in both heating and cooling modes will be decreasing over the time. TEM will pump or reject the heat from the experimental room rapidly at the initial stage of the experiment, then the heat transfer rate decreases as the conditioned room approaches to steady-state. However, the result was constraint to the experimental time which only carried out for 8 minutes.

Tian et. al. (2021) investigated the application of thermoelectric module in air cooler by using one single-stage module. Based on the prototype, air fluid was passes through the cold side of the module while the hot side was cooled by a water stream. It can be seen that the cooling capacity of the system was lower when the air flow rate was low. This is because the cooling effect of the TEM was stored in the heat sink and not transferred to the air fluid.

Therefore, higher air flow rate could enhance the heat transfer (cooling effect) between the cold side and the air fluid. For instance, the COP was increased from 1.9 to 2.4 when the air flow rate increased from 0.12 m³/h to 0.36 m³/h. Furthermore, the COP of the system was reduced significantly at higher input power despite of increased cooling capacity. Hence, the consideration between input power and cooling capacity must be taken into account when designing a system. The authors also studied on the cost analysis of the TEC, where \$1.40 per 1kWh was required for the tested prototype.

When designing a thermoelectric refrigerator, there are a lot of control factors such as supply voltage to the TEM and heat sink fans. Çaglar (2018) had developed a model to optimize the operations conditions of a portable thermoelectric refrigerator. The orthogonal fractional factorial experiment was applied in the study to investigate the relation between the voltages supply to outer fan, inner fan, Peltier module and ambient temperature. Using the optimized value, the refrigerator able to achieve a maximum COP of 0.351 when a 1 kg water was used as a cooling load. The temperature of the refrigerator decreased from 20 °C to -18 °C in only one hour. However, the COP of the system was decreasing over the time, from 0.351 to 0.011 after 1 hour, this was due to the COP will be decreased when the temperature difference increased. It is noteworthy that the author apply 12V operating voltage for the TEC1-12706 module as the optimum condition.

In the recent study, researchers also investigated the heat sink performance especially at the hot side of the TEM, because an efficient heat sink will contribute to the high performance of the module. Karwa et. al. (2017) had developed a water jet cooled heat sink with low thermal resistance of the TEM. The commonly used water-cooled sink is by passing through a water stream to the TEM instead of water jet. A 3D printed water jet heat sink was attached to the hot side of the TEM with constant heat load, the thermal resistance able to achieve as low as 0.025 K/W, whereas the common heat sink only around 5.0 K/W. With minimum thermal resistance, the performance of the TEM can be enhanced as the hot side temperature is reduced further.

2.4 Cascaded thermoelectric system

When the temperature difference across the hot and cold side of the TEM is large, the COP of cooling effect will be decreased (Sulaiman et. al., 2018). Therefore, multistage TEM is introduced to increase the performance of the TEM when the large temperature difference is required. A multistage module is usually formed by stacking two or more single-stage module with each other, so that one heat side of the module will be cooled by another cold side of the module.

The highest attainable temperature difference between the hot and cold side of TEM is subjected to the material properties and also the supply voltage. In order to achieve a lower temperature at the cold side, the TEMs are stacked up to increase the number of Peltier stage cooling effects (Aliabadi, Mahmoud, AL-Dadah, 2014). According to their studies, the cold side temperature of 3-stages module can reach up to 215 K (-58 °C) which is lower than 2-stages by 30K. However, the COP of 3-stages TEM is 0.12 while for the 2-stages is 0.22. In a cascading setup, the uppermost module will be cooled by the below module, where the heat will be transferred from the hot side of the upper module to the cold side of the below module. As a result, the uppermost module can achieve a lower cold temperature as the hot side temperature can be further cool down depending on the number of stages. On the other hand, the cooling capacity and COP of the TEM will be reduced when the number of stages increased. Therefore, the trade-offs between the cold side temperature and the COP of the TEM must be taken into account when designing the number of cascading stages.

To achieve the optimal cooling effect of the TEM, the input current must be regulated precisely as the Joule heating energy will affect the performance of the TEM (Belovski & Aleksandrov, 2019). The study investigated the performance of an actual 4-stages pyramid-style cascaded TEM at different value of current input. The maximum temperature difference across the TEM was achieved at the input current of 5 A (exceeds the maximum operating current of the module by 1.0 A), however, the optimal current to achieve the lowest temperature at cold side was 4A. This study is noteworthy in the fact that the maximum temperature difference across a TEM does not equivalent to the lowest temperature at the cold side. This might due

to the high temperature at the hot side will affect the temperature of the cold side to increase as well due to the thermal conductivity and the heat flux leakage between the stages of TEM, along with the Joule heating effect due to the high current supply.

Ma and Yu (2013) had studied on the performance of an alternative cascading thermoelectric cooler module configuration by simply joining two short-legged thermoelectric couples. Two couples are sandwiched between the ceramic plates and electrically connected in parallel while thermally in series. This configuration has the advantages of compact, single power supply, no interstage electrical insulating materials and reduced thermal resistances. In particular, the heat dissipated from the first stage can be completely pump to the second stage, thus enhancing the heat transfer efficiency. The authors also studied the effect of ratio between the length of two thermocouple legs to the cold side temperature of the module. Comparing the performance of the TEM with the study of Aliabadi, Mahmoud and AL-Dadah in the section above, both of the configurations able to achieve a maximum COP of about 0.2 at the cold side temperature of 245K. This has proven that the directly connected TEM can perform well as same with the pyramid modules design. However, further investigation and physically prototyping should be carried out to convince the performance of alternative TEM design.

Karimi, Culham and Kazerouni (2011) had investigated on the effect of multi-stage thermoelectric cooler (pyramid-style) to the overall COP of the system. It was clearly shown that the ratio of contact area between the cold surface to the hot side of the subsequent TEM directly affect the performance of the thermoelectric system. When the ratio of contact area increased, the COP of the system was decreased. For instance, the maximum achievable COP of the 5-stages thermoelectric was 3.0 (ratio 1.0) and 1.6 (ratio 1.4). This was due to the thermal resistance of the heat sink was increasing with the ratio of contact area. It can be concluded that in order to achieve the higher COP, the heat sink thermal resistance at the last stage must be as low as possible to dissipate the heat easily. On the other side, when the number of stages increased, the maximum attainable COP was increased as well, which was 3.2 at 8-stages. However, that was achieved at the low current region (1–3 A), the COP was dropped significantly with more cascaded stages at high current

input. For instance, it dropped to 1.1 only at current input of 8.0 A for the 8-stages TE cooler. Therefore, the optimal operating current for the TEM and the desirable COP of the system must be evaluated properly to achieve optimum performance.

The comparison of energy, exergy and exergoeconomic analysis between single-stage and two-stage thermoelectric devices had been conducted by Nami, Nemati, Yari and Ranjbar (2017). Two-stage thermoelectric was apparently had the higher maximum attainable COP value for both cooling and heating mode, despite of three temperature difference boundary conditions. However, it can be seen that the effective range of the current was wider for single-stage especially at higher current region, as shown in Figure 2.2. The COP of the two-stage model started to decline drastically when the supply current beyond its optimal range. This might due to the power consumption was dominating over the cooling/heating effect of the thermoelectric. Nonetheless, it is noteworthy that the two-stage thermoelectric able to reduce the power consumption and increase the COP in both heating and cooling effect under its optimal operating range. The exergy analysis also confirmed that two-stage thermoelectric had higher efficiency.

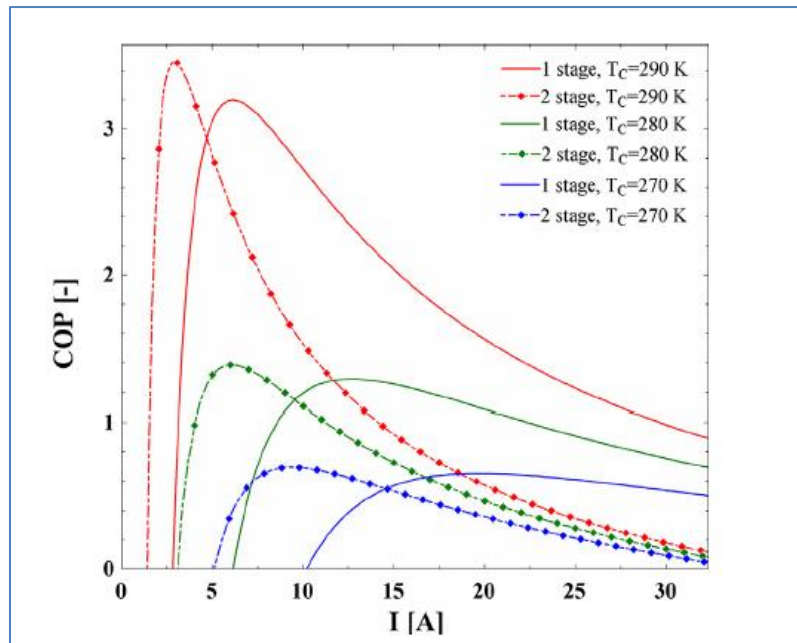


Figure 2.2: COP of cooling mode versus current for single- and two-stage thermoelectric at different cold side boundary conditions (Nami, Nemati, Yari & Ranjbar, 2017).

Most of the single stage TEMs available on the market are capable to operate for up to 70 K temperature difference only. Parashchuk et. al. (2021) had developed a six-stage TEC that can reached 140 K (-133 °C) at the cold side for the application of mid-infrared sensors and lasers. In their designs, customized-made two-stage ultra-low temperature TEM was cascaded with a commercial four-stage TEM. As a result, the maximum temperature difference between the first stage to the last stage can reach up to 150 K from ambient temperature. It can be seen that the multi-stage TEM provides higher heat pump capacity and cooling capability, at the same time with lower cold side temperature.

Kamasi et. al. (2020) had analysed the performance of the 2-stage and 3-stage cascaded TEM with pulse width modulation (PWM) method. In their experiment, the similar Peltier modules were stacked with each other using thermal paste and the hot side was cooled by the water block. Although the 3-stages TEC could achieve higher temperature difference and lower cold side temperature, the variation between 2- and 3-stages was very small only. For instance, the cold side temperature for 2-stages was 14 °C and 3-stages was 12 °C. Therefore, the extra Peltier module and extra power consumption that needed to get the extra temperature difference have to be considered properly when designing the system. Nonetheless, the result is limited to 50% duty cycle of PWM only, the authors did not adequately look into the performance of TECs when operating at higher duty cycle which might have different result.

In order to further enhance the temperature drop across the two-stage thermoelectric cooler, pulse current is introduced to supply the current for TEM instead of constant current supply. Gao et. al. (2017) proved that by simultaneously supplying pulse currents to the two stages in separately source could make the two-stage TEM achieve lower cold side temperature, which was from 257.08 K to 229.10 K. It should be noted that the pulse current at here is elevated to the optimum steady-state current of the 2-stage TEM (as “low” state), then a ratio of current is amplified (as the “high” state). By using this method, the Peltier cooling effect is more significant enhanced before the Joule heating effect take place when a sudden high current is supplied, thus it could further reduce the cold end temperature. Furthermore, the authors also

mentioned that the pulse width at the hot stage should be shorter than the cold stage, with 0.45s and 0.60s respectively, so that the cold temperature is lower and has longer holding time.

Li et. al. (2019) had studied the performance of a commercial two-stage TEC with pulse current operation, which was TEC-12704. The study was similar with the Gao et. al. as described above, but experimental analysis was carried out instead of numerical study. They proved that the pulse current able to further reduce the cold side temperature as compared to the steady-state, which was from 236.65 K to 232.90 K (-36.35 to -40.1 °C). The optimum cold side temperature also achieved with pulse period of 6s.

As the COP of the multi-stage cascaded TEM is always dropped at higher stage, Provensi and Barbosa (2020) had studied the performance of the air stream cooler with horizontally-stacked configuration of TEMs in a rectangular duct. The outlet air stream temperature was cooled down by 8 °C (25 °C to 17 °C) and the maximum attainable COP was around 2.5 for 3 – 12 number of TEMs at low thermal load region (less than 60 W). It demonstrated that the COP dropped at higher cooling load regardless of any number of TEMs, this might mainly due to the Joule heating effect where the electrical power is dissipated as heat. Besides, the horizontal stacking configuration also showed an advantage over the pyramid style cascaded TEM with the same number of modules. It can achieve the COP by 60% more than cascaded TEM at moderate to high cooling load (100 - 200 W).

2.5 Solar-Thermoelectric system

Solar energy can be utilized to power up the thermoelectric modules as it provides a clean and emission-free energy. Abdul-Wahab et. al. (2008) had designed a portable solar thermoelectric refrigerator to be used in the rural areas where the electricity supply is limited. A prototype with 64 solar cells, 10 TEMs and 10 heat sinks was built with a 23 x 18 x 32 cm³ container. The temperature of the refrigerator was able to be reduced from 27 °C to 5 °C in 44 minutes with the COP of 0.16. Differ from the previous studies above, the size of TEM used by the author was small with dimension of 15 x 15 x 4.3 mm only (typical dimension 40 x 40 x 4 mm), however, the performance of the refrigerator was outstanding as 10 TEMs were used. A major drawback of this

setup is it required high power supply with 111 W. Consequently, the photovoltaics solar cells were connected in series and parallel to increase the maximum potential difference and current at the final output terminal.

For a solar-powered thermoelectric refrigerator system, the condition of the weather is an important aspect as the irradiance from the sun directly impact on the power supply to the TEM. He et. al. (2013) had studied on the performance of the solar thermoelectric system throughout the whole day, from morning to afternoon. The average COP obtained by the system was 0.60. The highest power output of 35W from the solar cells was reached at noon around 12:00 PM, however, the lowest temperature at the cold side and experimental room was achieved at 10:30AM, with values of 9 °C and 16 °C respectively. This might due to the heat leakage from the hot side of TEM in the experimental room as it was not completely isolated while it reached the highest temperature at noon. Besides, the heat transfer between the experimental room and environment might cause the cold room temperature to rise as well. However, the approach was not in the ideal way as the heat from the hot side of the TEM was not isolated completely from the experimental room. From this study, it is noteworthy in that the power generated from the solar cells is varying in a parabolic pattern throughout the day. Therefore, the power generated must be regulated properly to make sure that the TEM will not be overheating and affect its performance.

In order to make the solar-powered thermoelectric refrigerator could operate in day and night, Rahman et. al. (2020) had integrated a battery storage system to the refrigerator, along with the charge controller and DC-DC converter. The results showed that the performance of the refrigerator at day time had the almost same result with the battery-powered system during night time. However, the lowest temperature achieved in the cold chamber was about 19 °C only, with the COP of 0.306. The result is not convincing in that the cold temperature is not enough to be applied for the refrigerator system. Nonetheless, the authors had provided an important insight that the TEM cold side temperature will be increasing significantly when the hot side was enclosed in a chamber and this will negatively impact on the performance of the cooling chamber. As the accumulation of the waste heat energy in the hot

chamber, the hot side temperature will be increasing higher and thus the cold side.

Saidur et. al. (2008) had focused on the performance of photovoltaic system with battery bank to power up a thermoelectric refrigerator. The battery bank was able to supply the power to the refrigerator for 3 autonomous powering days without additional solar power, while maintaining cold chamber temperature at around 5 °C. It was an outstanding result in terms of the TEM efficiency, chamber insulation and steady power supply. In their design, 4 solar modules with 100W each and 4 lead acid type batteries (100Ah) were used to power up a 22W thermoelectric fridge. Besides, a solar charge controller was used to prevent the battery from overcharging and overheating which might contribute to the permanent damage. The power supply system was sufficiently enough for a such small electricity consumption of thermoelectric refrigerator. However, the design does not adequately account for portable usage as the whole setup is bulk in size due to the high-power storage system.

Dai, Wang and Ni (2003) also analysed the performance of a solar-driven thermoelectric refrigerator during daytime. In overall, the system able to maintain the chamber at 5-10 °C with COP of about 0.3. It is found out that the COP of the fridge was decreasing with the increasing of solar insolation rate, obtaining minimum COP of about 0.20 at 12.00 PM. This was due to the cooling capacity (Q_C) dropped slightly when the solar insolation rate increased. Furthermore, the study also highlighted that the hot side temperature must be kept as low as possible to achieve the optimal COP, Q_C and performance of the refrigerator.

Table 2.1: Comparison of different solar-driven TE refrigerator

	Rahman et. al.	Saidur et. al.	Dai, Wang & Ni
Solar cell	4 units 5 W	4units 100 W	2units 0.4 m ² (13%)
Battery	48 Ah 12V	4 units 12V, 100 Ah	100 Ah
TE refrigerator	5 units 1.17W/unit	22W	45 W, 12 V
Cold side temp. (min)	10 °C	2 °C	5 °C
Chamber temp. (or water)	19 °C	6 °C	10 °C
COP	0.306	-	0.30

2.6 Self-driven thermoelectric model

The self-driven TEG-TEC system is a significant useful device when the cooling effect is required but without power supply. It can use the waste energy or solar energy to generate the electricity. According to Lin et. al. (2019), when the two stage TEG-TEC system was connected in series current connection, it had shown a low cooling capacity and low performance. They proposed a new design by using two single-stage TEGs to power up a two-stages TEC. From the results, the new design yielded a higher cooling capacity and also a larger temperature difference across the TEC. It is proven that the separate TEG power configuration can provide a better cooling effect on the TEC. Besides, the study also performed an optimization on the ratio of couples in between TEGs (TEG 1 to TEG 2) and TEGs to TECs. This is due to the number of thermoelectric couples used to power up the two stages of TEC will affect the overall performance of the system also. Hence, it is necessary to take into consideration when designing a TEG-TEC system.

2.7 Summary

From the previous literature studies, it can be concluded that the thermoelectric module is a promising solution to replace with the conventional vapour compression refrigeration cycle. It can be used for the portable mini fridge due to its simplicity of operation and small in size. However, the application of TEM in a hybrid storage system is still limited and scarce to be discussed in the past research. The parameters that direct affect the performance of the TEM have been discussed in the section above, such as supply current, number of cascaded stages, electrical connection setup, solar-powered system and the analysis model for the thermoelectric system as well. Therefore, the latest technology and knowledge attained from the literature will be practiced to develop a hybrid storage system for cooling and heating by using the TEM.

CHAPTER 3

METHODOLOGY AND WORK PLAN

3.1 Introduction

The section below describes the workplan for the entire project in detailed. The main objective of the project is to develop a hybrid storage system by using the thermoelectric modules. The technical knowledge and latest technology learned from the previous section are applied to find the optimal solution for the design. The project can be classified into two stages; simulation to get the optimal design and the prototyping stage to verify the result.

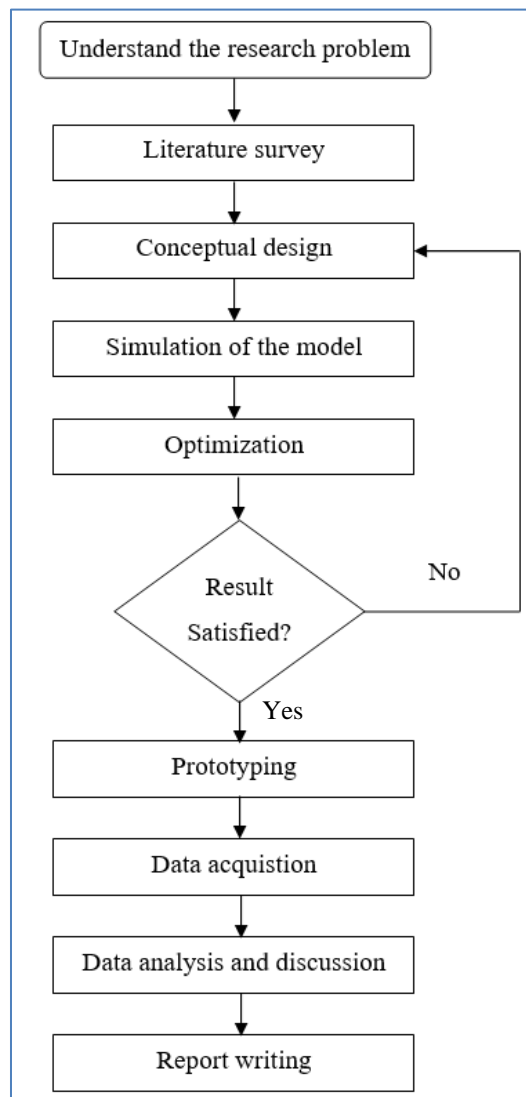


Figure 3.1: Flow chart of the project

3.2 Simulation model

In this study, the cooling and heating effect of the chamber is achieved by the heat transfer from the thermoelectric module. The fans and heatsinks are attached to the thermoelectric module so that the heat transfer rate could be increased. Therefore, ANSYS software will be used to simulate the thermal condition inside the chamber. ANSYS's Fluid Flow (Fluent) model will be the best solution for this study, as it able to perform the modelling of Computational Fluid Dynamic (CFD) and deal with the temperature distribution.

3.2.1 Setup of ANSYS software

As this simulation study is mainly focus on the air flow and temperature distribution inside the chamber, the internal dimension of the chamber is sketched out. There are four inlets at the side of the chamber which represents the location of thermoelectric module. Figure 3.2 shows the geometry input at the ANSYS with four inlets. The rectangle box itself represents the fluid (air) inside the chamber without wall thickness, while the inlets are the cold air that flowing out from the fans of thermoelectric module.

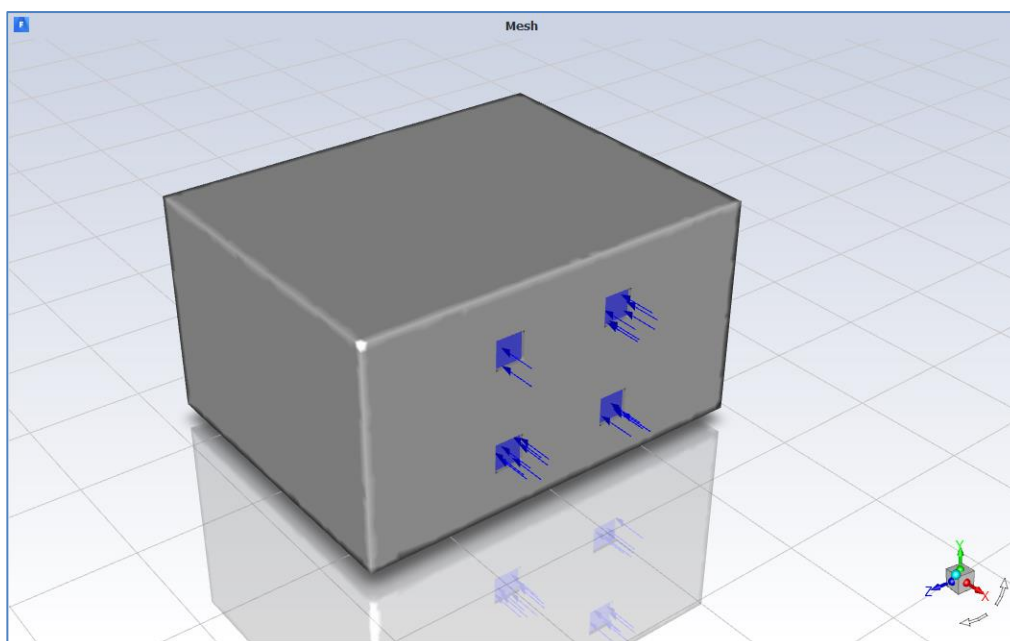


Figure 3.2: Geometry of insulation chamber in ANSYS with four inlets

By referring to the datasheet of the small 40 mm computer fan as shown in Figure A-1, the calculation can be performed to get the air velocity of the fan at the inlets. The value obtained is 1.875 m/s which is approximately equal to 2.0 m/s and this value is used as a reference for the simulation model. Besides, as the cold side of the module will attach to the heatsink and fan, the air velocity flowing out from the fan has a temperature that closes to the cold side of the module. The module can easily get below 0 °C (273 K) at the cold side, for example, the TEC1-12706 that used in this study can get the lowest temperature at -5.34 °C. As a reference in the simulation study, the inlets are set to 2.0 m/s with 273 K cold air blowing to the chamber.

In addition, a heat source is included in the simulation model, which is a constant heat generation inside the fluid to represent a heat load to the chamber. Without the heat load in the simulation, the whole fluid will reach steady state at the temperature that same with the inlet air temperature at 273 K. Therefore, a 500 W of heat load is considered in this simulation setup as a consumption of actual working environment. The heat load is divided by the volume of the chamber (fluid), the result obtained is 7500 W/m³ which is a constant energy source in the simulation.

Moreover, the thermal boundary condition at the wall is set as “via system coupling”. There is a heat source within the fluid domain, therefore the thermal condition at the wall should be depending on the heat source as well. The total amount of heat that added or removed from the system can be observed through the thermal condition at the wall. Temperature distribution profile at the wall will be observed to evaluate the performance of the chamber and design. Table 3.1 below shows the summary of the ANSYS simulation setup.

Table 3.1: Details of ANSYS setup

Analysis system	Fluid flow (Fluent)
Model	Viscous (SST k-omega) Pressure-based with gravitational acceleration Steady state
Material	Fluid (air) Wall (aluminium)
Cell zone condition of fluid	Constant energy source (7500 W/m ³)
Boundary conditions	Inlet <ul style="list-style-type: none"> • 2m/s at 273K Wall <ul style="list-style-type: none"> • No slip • Thermal condition via system coupling
Solution method	Scheme: Coupled Gradient: Least Squares Cell Based Pressure: Second Order Momentum: Second Order Upwind
Number of iterations	1000

3.3 Experimental design

An actual prototype is developed to examine the performance of thermoelectric module under actual working environment. Two chambers with simple insulation material are designed to test the cooling and heating effect of the thermoelectric module. There are total of three operation modes in this study, which are cooling mode, heating mode and simultaneous cooling and heating mode.

3.3.1 Cooling mode

Figure 3.3 shows the actual prototype of cooling chamber. The cold side of the Peltier module is located at the internal volume of the polystyrene box. Meanwhile, the hot side of the module which is the larger size of heatsink, is located at the outside and exposed to the ambient. There are total of four Peltier modules.

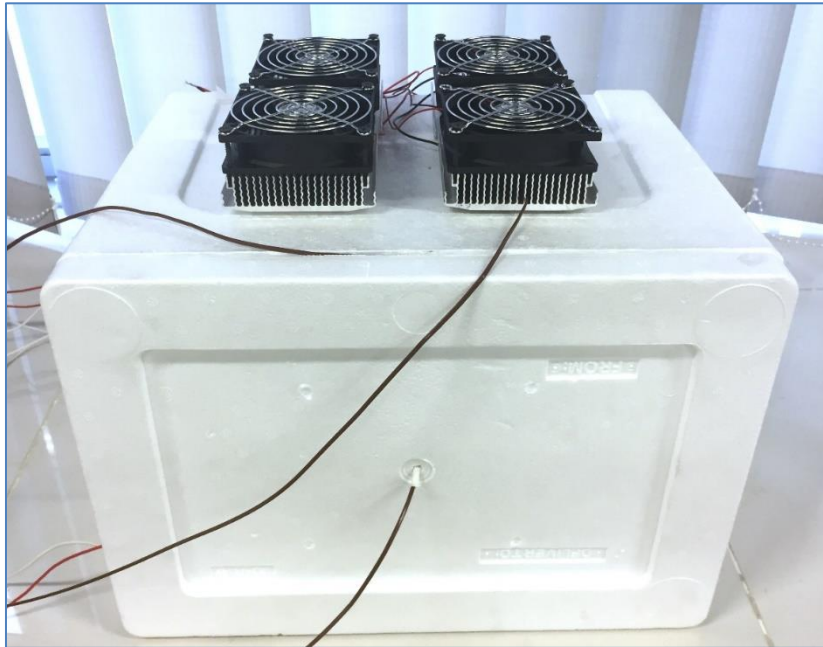


Figure 3.3: Chamber design for cooling mode

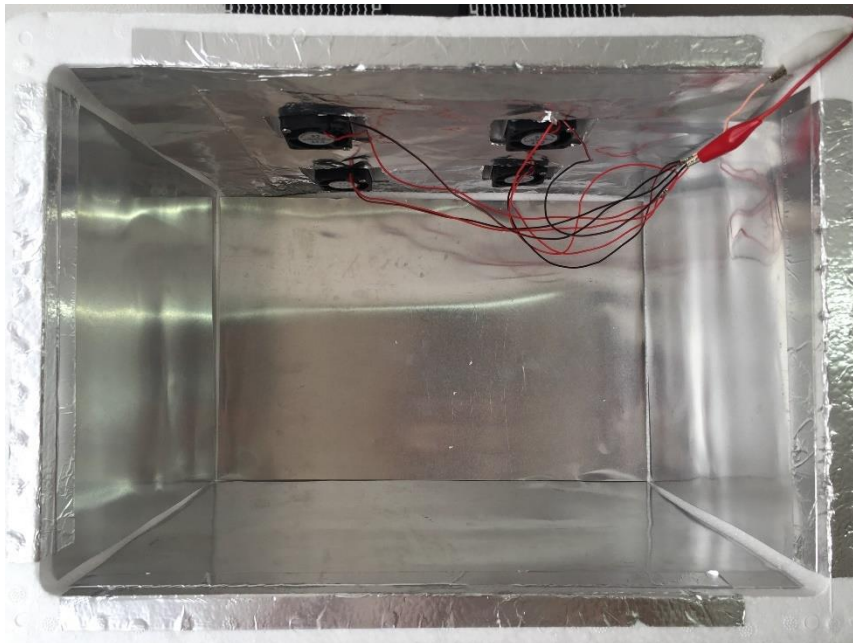


Figure 3.4: Internal of the chamber with layered aluminium sheet

3.3.2 Heating mode

Figure 3.5 shows the prototype of heating chamber. In this configuration, the hot side of the Peltier module is enclosed in the polystyrene box while the cold side is exposed to the ambient. There are total of four Peltier modules as well.



Figure 3.5: Chamber design for heating mode

3.3.3 Simultaneous cooling and heating mode

Figure 3.6 shows the schematic drawing of simultaneous cooling and heating mode. Two chambers are attached to each other side-by-side. The lower part is cooling chamber whereas the upper part is heating chamber. Four Peltier modules are inserted in between the two chambers. The actual prototype is shown in Figure 3.7, note that one side of the lid of heating chamber is opened for a 2 cm gap. This allows some evacuation for the accumulated thermal energy inside the chamber, this would help to maintain an equilibrium temperature state between the cooling and heating chambers.

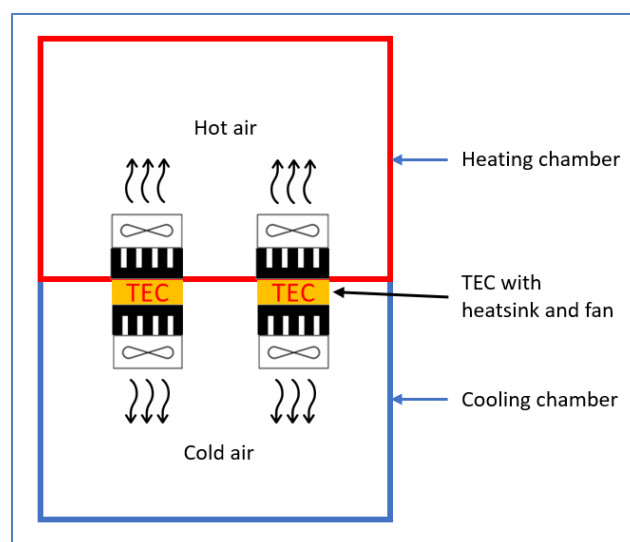


Figure 3.6: Schematic drawing of simultaneous mode

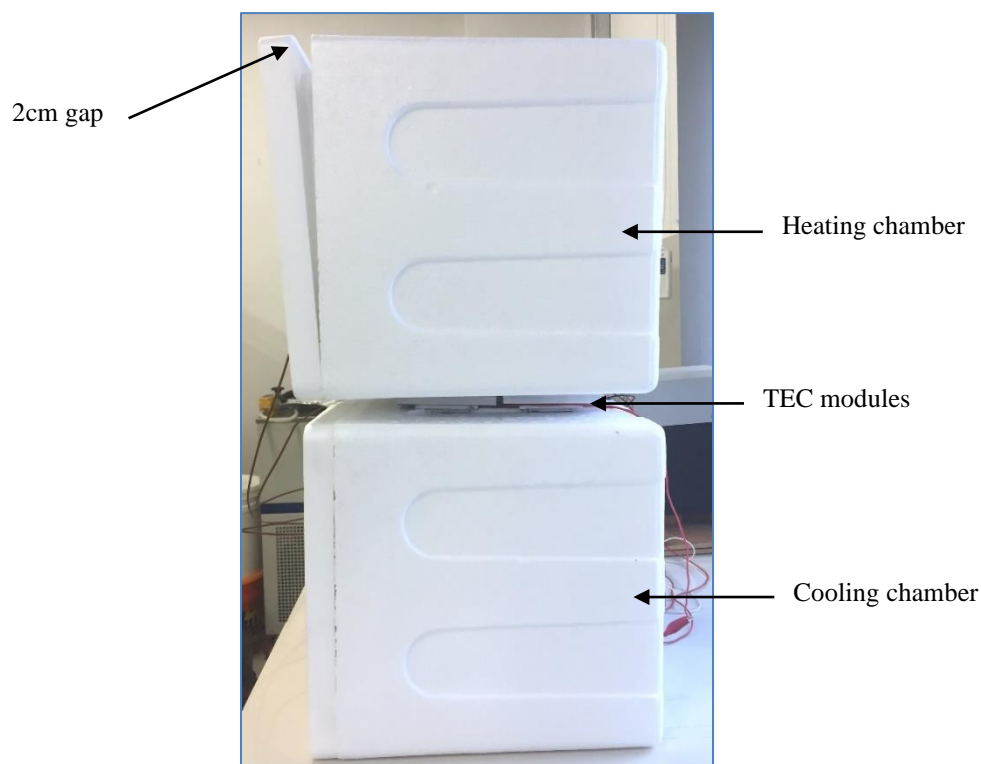


Figure 3.7: Chamber designs for simultaneous cooling and heating mode

3.3.4 Apparatus and equipment

3.3.4.1 Peltier module

Thermoelectric module, also known as thermoelectric cooler (TEC) or Peltier module, as it applies the Peltier effect to create heating and cooling effect on two ceramic plates. In this study, TEC1-12706 is used as the heat source and cooling source to develop the hybrid storage system. It is a single stage module, with maximum operating current at 6.0 A and 127 couples of p-n junction semiconductor. The dimension of it is 40 mm x 40 mm x 3.75 mm, as shown in Figure 3.8.

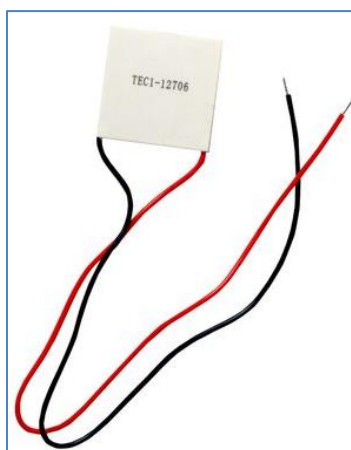


Figure 3.8: Thermoelectric module with part number TEC1-12706

3.3.4.2 Heatsink

Heatsink is a passive heat exchanger with arrays of fins to increase the effective surface area that expose to the cooling medium. As the thermal energy always flow from a high temperature region to low, the heatsink carries the heat energy away from a heat source to itself via Fourier's law of heat conduction. Then, the thermal energy will be transferred to its surrounding by the effect of convection. As referring to the equation of heat convection, the rate of heat transfer is directly proportional to the surface area of the system. Therefore, heatsink able to increase the total surface area that expose to the cooling fluid such as air to reject the heat from the Peltier module. Two heatsinks are used in each Peltier module, one with dimension of 120 x 100 mm at the hot side and another one with 60 x 45 mm at the cold side. The hot side of the module require larger heatsink as the amount of heat generated at the hot side is much larger than the amount of heat absorbed at the cold side.

$$\dot{Q} = hA\Delta T \quad (3.1)$$

3.3.4.3 Fan

To further increase the heat transfer rate of the TEC, fans are attached to the heatsink at both hot side and cold side. The fan induces a forced convection to the heat sink so that the flow rate of the cooling medium is increased. When the velocity of cooling fluid is increased, the convection heat transfer rate can

be increased as well. A 9 cm computer fan is attached to the heatsink of the hot side while another smaller 4 cm computer fan at the cold side.

3.3.4.4 Thermal paste

During assembly of Peltier module, a thermal paste is applied on the ceramic plate of the module at both sides. It is a thermal conductive material but electrically insulated. The main function of thermal paste is to eliminate any air gaps in between the heat sink and the heat source. This would help to maximize the heat transfer and heat dissipation of the Peltier module to the heat reservoir.

3.3.4.5 Polystyrene box

Polystyrene box is one of the best thermal insulation materials and suitable to build as a chamber in this study. It is also inert to any chemical reaction and has high melting point. According to Sastri (2010), the melting point of polystyrene is around 270 °C and the glass transition temperature is 100 °C. The strength of the polystyrene box will only go down when it reaches 100 °C and become soften. However, the Peltier module and the heatsink does not reach at this temperature, hence it is safe to implement it as an insulation chamber. Two 25 Litres of polystyrene boxes with dimension of 379 x 252 x 267 mm are used as the insulation chamber in this study.

3.3.4.6 Aluminium sheet

To further enhance the heat transfer rate inside the chamber, the internal wall of the polystyrene box is layered with thin aluminium sheet. The thermal conductivity of the air is very low with 0.0025 W/mK only, therefore the heat transfer in between the Peltier module and the air inside the chamber mainly depend on the heat convection. With the aluminium sheet as the internal wall of the chamber, the surface temperature of the aluminium sheet will be close to the heating/cooling source as it has a very high thermal conductivity at 247 W/mK. As a result, the heat transfer from the aluminium sheet to the air could be achieved by the heat convection effect, so that there are two ways of heat transfer inside the chamber. The aluminium sheet used in the design has a

thickness of 0.3 mm only. It is a thin sheet with bulk dimension of 4 ft x 5 ft. It is cut into smaller pieces so that it is fit to the inner wall of the polystyrene box.

3.3.4.7 DC power supply

All of the components in the prototype such as fans and Peltier module require DC power supply to operate. Two power supplies are used, which are GW Instek GPC-3030 and TTi QPX600D with maximum power output 375 W and 600 W respectively. The smaller power supply is used to power up the fans as it only requires small current at 0.2 A per computer fan. On the other side, the Peltier module will draw a large current at around 3.0 A per module, hence it is powered by the TTi power supply as it can supply up to 50 A.



Figure 3.9: GW Instek GPC-3030 power supply



Figure 3.10: TTi QPX600D power supply

3.3.4.8 Data logger

To measure the temperature of the prototype and Peltier modules, a temperature measurement data logger is used, which is Graphtec midi logger GL840. It has multiple input ports with maximum 20 inputs and fast response with maximum sampling interval of 200 ms. The data can be recorded in excel csv format to obtain the temperature profile of the prototype.



Figure 3.11: Graphtec midi logger GL840

3.3.4.9 Thermocouple

Thermocouple is a temperature sensor that made up of two different metal wires and joined at one end. When the temperature at the metal junction is changed, a voltage is created and this voltage is interpreted by data logger to translate it into temperature reading. It is also working based on the Seebeck effect which similar to the thermoelectric generator. In this experiment, thermocouple type-K is used to measure the temperature. The yellow wire is the positive terminal while the red wire is negative terminal. It can measure the temperature ranging from $-200\text{ }^{\circ}\text{C}$ to $1250\text{ }^{\circ}\text{C}$, which is sufficient to measure the temperature in this study.



Figure 3.12: Thermocouple type-K

3.3.4.10 Sub-assembly of Peltier module

Figure 3.13 shows the assembly of TEC1-12706 with cooling kit, including heatsink and fan at both hot side and cold side. The TEC1-12706 is embedded in an insulation gasket as shown in white colour pad in the picture. It helps to prevent the heat flow from the hot side of the module. It also prevents the water that produced by condensation at cold side to get into the modules which might cause short circuit.

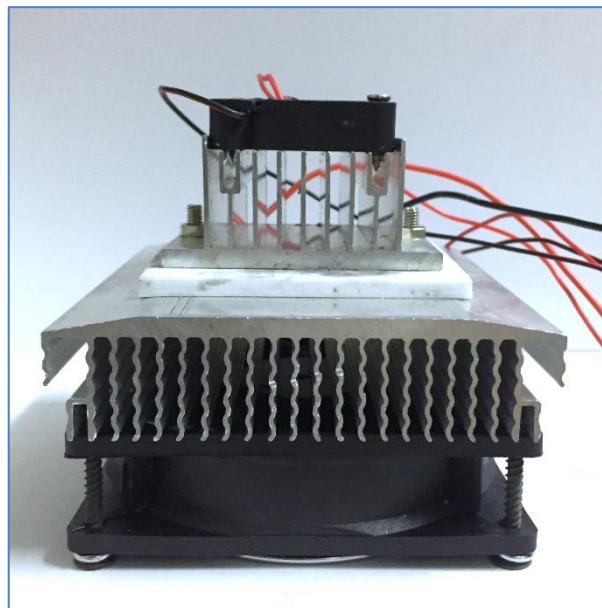


Figure 3.13: Sub-assembly of Peltier module

3.3.5 Preliminary testing on TEC1-12706

Under Peltier effect on the thermoelectric module, the temperature of the cold side will keep decreasing when the current is increasing. However, there is a limitation on the module where the Joule heating effect will overtake the Peltier effect. At that moment, the cold side temperature will rise up and become warmer. Therefore, a preliminary testing is performed on the TEC1-12706 to find its optimum operating current. Table 3.2 below shows the temperature response of the Peltier module at different current. The power supply is run at constant current setting. From the result as shown Figure 3.14, the lowest temperature obtained is $-5.34\text{ }^{\circ}\text{C}$ at 3.0 A. When the supply current beyond 3.0 A, the temperature at the cold side start to rise up. Therefore, 3.0 A is selected to be the operating current of TEC1-12706 in this study.

Table 3.2: Performance of TEC1-12706 under different current

I (A)	V (V)	T_c (°C)	T_h (°C)	DT (T_h-T_c)
1.0	3.98	11.04	28.96	17.92
1.5	5.64	4.95	31.09	26.14
2.0	7.12	0.83	33.20	32.37
2.5	8.63	-2.89	36.25	39.14
3.0	10.16	-5.34	38.91	44.25
3.5	11.81	-2.97	43.86	46.83
4.0	13.70	4.38	51.3	46.92
4.5	15.65	4.41	55.46	51.05
5.0	17.6	5.60	63.6	58.00

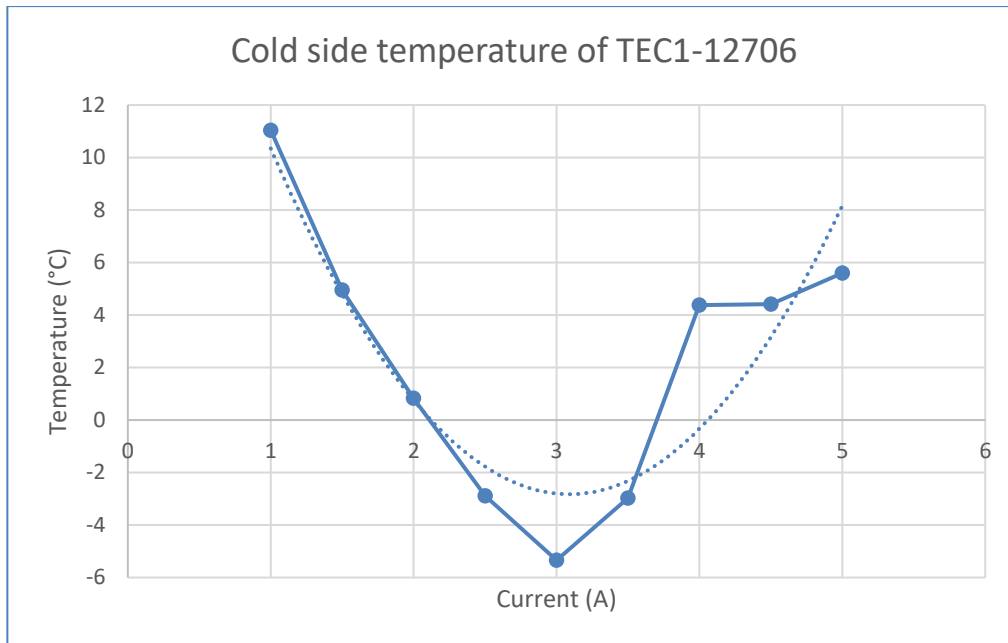


Figure 3.14: Graph of TEC1-12706 cold side temperature at different current

3.3.6 Circuit diagram

After the optimum operating current for Peltier modules has been determined, the circuit diagram of the prototype can be drawn out. As mentioned above, TTI QPX600D which is the high wattage power supply is used to power up four TEC1-12706. It has two individual power outputs, hence one power output is used to power up two TEC. Figure 3.15 and Figure 3.16 shows the comparison between series and parallel setup for two TEC. For instance, one TEC1-12705 will draw 3.0 A and 10.0 V. The total power supplied to the modules will be same but the connection wires in parallel setup will draw more current at 6 A. The wire will get hot easily and even burn, hence the series connection pattern is opted in the final design. The power supply is run at constant current mode as the current is more dominant in Peltier effect.

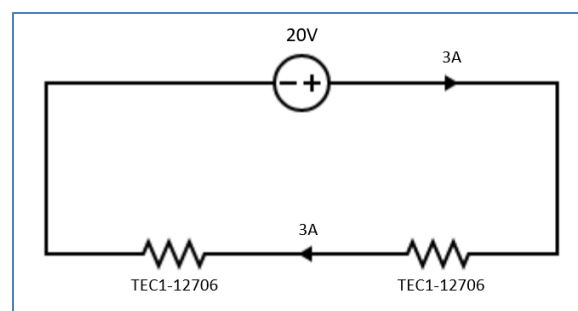


Figure 3.15: Series connection of two Peltier modules

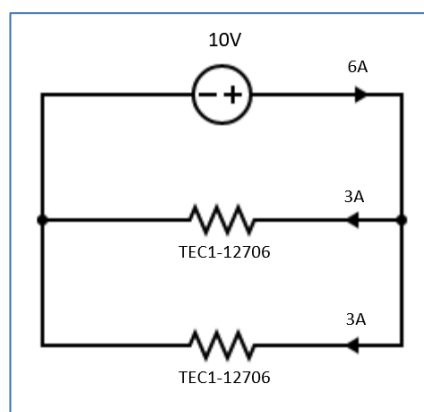


Figure 3.16: Parallel connection of two Peltier modules

On the other side, the GW Instek GPC-3030 is used to power up the computer fan on the heatsinks. There are also two individual power outputs, hence one output is used to power four units of 9 cm computer fan, whereas another output is used to power four units of 4 cm computer fan. Two different power outputs are applied as the smaller computer fan draw slightly lower current than bigger one, the 4 cm computer fan only consume 0.1 A while the 9 cm consume 0.2 A. The parallel connection setup is selected for computer fans, as the total current draw is very small at 0.8 A. The power supply is run at constant voltage mode because the computer fan requires high voltage rather than high current.

In total, there are four individual circuits that uses to power up four units of Peltier modules, four units of 9 cm computer fan and four units of 4 cm computer fan. The circuit diagram is summarized as shown in Figure 3.17.

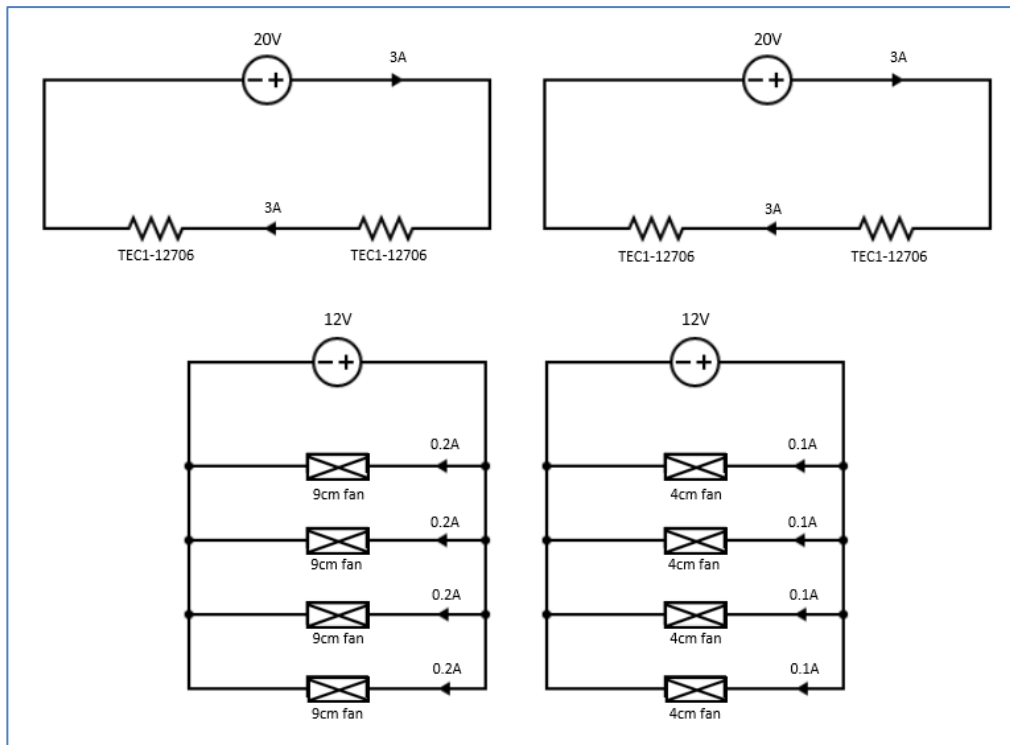


Figure 3.17: Circuit diagram for four individual power outputs

3.4 Summary

The ANSYS simulation model is performed to study the capability of TEC in cooling down a given heat load. It is done by setting the air temperature blowing out from the modules as input at the simulation model with a heat load apply to it. After the simulation result is obtained and satisfied, a prototype will be built to test the performance of TEC. Polystyrene box is used as the insulation chamber and covered with aluminium sheet at the internal wall. With the determination of optimum working current for TEC, the circuit diagram is constructed and analysed. After that, the prototype starts to operate and the temperature is recorded to study the performance of TEC. Three operating mode is conducted in this study, which are cooling mode, heating mode, and simultaneous cooling and heating mode.

CHAPTER 4

RESULTS AND DISCUSSION

4.1 Introduction

This section will discuss the result of simulation model to prove the design concept. Besides, this section also analyses the actual prototype performance of thermoelectric module when it is working under cooling mode, heating mode or simultaneous cooling and heating mode. The temperature of the chamber, heat sink of both cold side and hot side are recorded throughout the operation of the prototype. The COP at each operation modes is discussed as well to identify the effectiveness of the system.

4.2 Simulation model

ANSYS fluent model is used to identify the cooling load of the system with a heat source. First of all, the grid dependency test is conducted to identify the optimum mesh size for the geometry model. The analysis is done by varying the mesh size of the model from coarse to finer size. When the solution results for each run does not change significantly, it indicates that the simulation result is not dependent on the mesh size anymore. Table 4.1 below shows the results of 8 iterations from 50 mm to 10 mm mesh size. Figure 4.1 also demonstrate the graph of grid dependency test in a clearer view.

From the result, the wall temperature does not change significantly when the body sizing is 10 mm with 168 116 mesh elements. Moreover, the graph is stable after this point which indicates that the simulation results is not dependent on the grid size anymore after this step. Therefore, the 10 mm body sizing with total 561 571 mesh elements is chosen to perform the simulation procedure.

Table 4.1: Grid dependency test with 8 iterations

Design point	Body Sizing [mm]	Mesh Nodes	Mesh Elements	Wall temperature (K)
DP 0	50	1102	4997	322.81
DP 1	45	1409	6563	320.27
DP 2	40	1924	9185	322.52
DP 3	35	2748	13622	321.82
DP 4	30	4200	21213	319.38
DP 5	25	7056	36600	328.83
DP 6	20	13146	70308	321.79
DP 7	15	30733	168116	324.40
DP 8	10	99552	561571	324.55

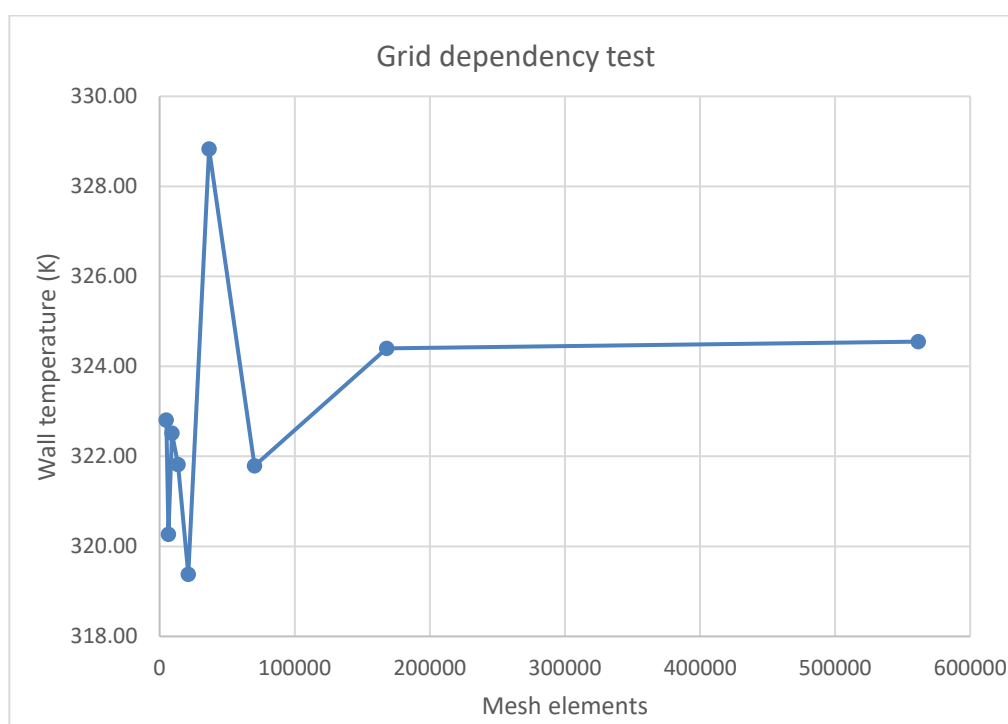


Figure 4.1: Graph of grid dependency test with wall temperature vs mesh elements

This test is able to determine an optimum mesh size to give a better result with less time as compared to a finer mesh. Although the finer mesh would calculate a solution that is almost equal to the actual solution, it will require a very long time to complete the simulation. Therefore, this grid

dependency test provides an ideal mesh size that would give an appropriate result with optimal timing. Figure 4.2 shows the finalized grid model for the simulation with 10 mm body sizing.

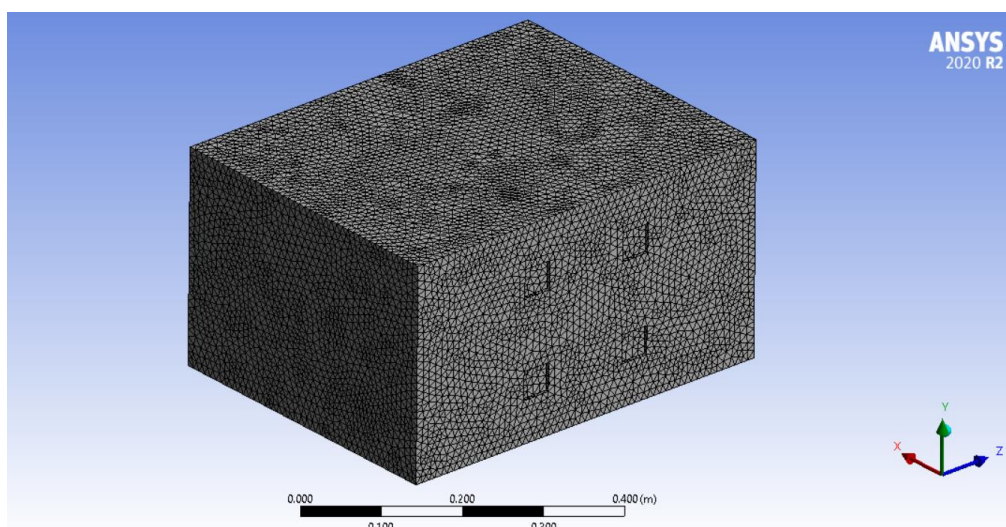


Figure 4.2: Finalized grid model with 10 mm body sizing meshing

The result as shown in Figure 4.3 presents the temperature distribution on the wall of the chamber. With a constant heat load within the fluid, the wall temperature still able to main at a range of 295.47 K to 328.78K. Although the temperature does not fully equal to the inlet temperature at 273.0 K, the system is still able to cool down the heat source of the fluid.

If the inlet temperature is set as ambient temperature at 300K, the temperature of the fluid will go higher as there is no cooling effect on the fluid. The testing result shows that the wall temperature will be ranging from 323.26 K to 352.50 K if the inlet temperature is 300 K, as shown in Appendix. Therefore, with the inlet temperature of 273 K, it proves that the model configuration able to cool down the 7500 W/m^3 heat source of the fluid. The four inlets design will be adapted to implement on the actual prototype.

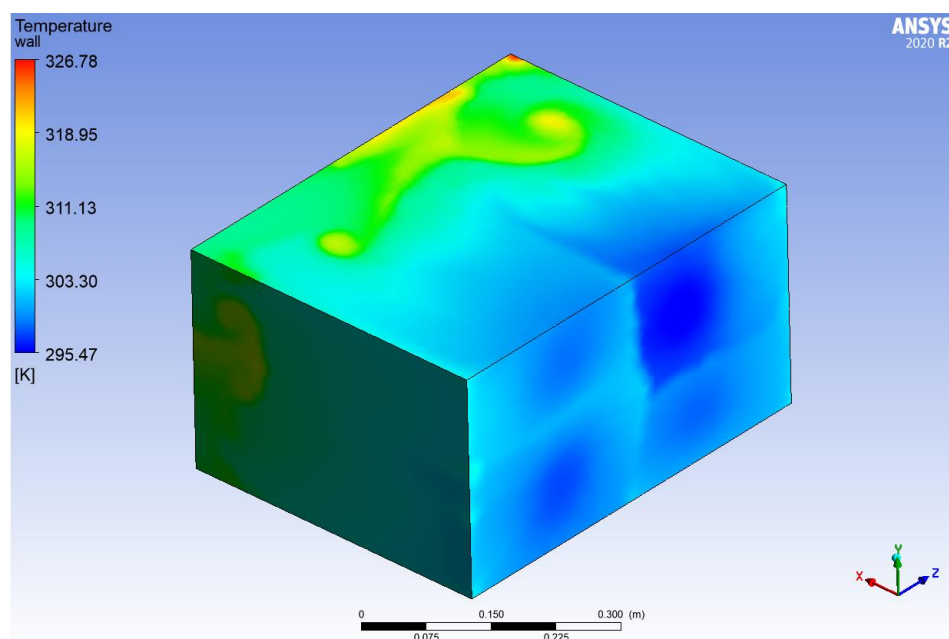


Figure 4.3: Temperature distribution on the wall of the fluid domain

Moreover, this simulation result also shows the overview of the temperature distribution within the chamber. From the Figure 4.3, the coolest region of the chamber is directly at the front of the inlets. It shows the flow pattern of the fluid when the fans are enclosed in the chamber and the location at which the lowest temperature will achieve. Therefore, the 2 x 2 arrangement of Peltier modules (total 4 units of TECs) will be used in the prototype as the best position to cool down a chamber.

After the prototype is built, experiments are performed to evaluate the actual performance of the Peltier modules.

4.3 Cooling mode

When the prototype is running at cooling mode, the air temperature inside the chamber able to cool down from room temperature at about 25.0 °C to 5.89 °C in 30 minutes. This temperature is very close to the household fridge and it is capable to store fresh foods such as vegetables, fruits and beverages.

TEC has a very fast response in creating a temperature difference between its hot side and cold side. Once the power is turned on, the cold side temperature on TEC able to reach about 3.0 °C while the hot side temperature at 37.0 °C in 5 minutes. The temperature drop at the cold side is exponential and achieve an equilibrium state after certain period as shown in Figure 4.4.

After 15 minutes of operation, the cooling chamber almost reaches its equilibrium with temperature of about 7 °C. After that, it slowly decreases and the minimum temperature inside the chamber is 5.89 °C.

At the equilibrium state, the cold side temperature of the TEC which represents by the temperature of the heatsink, is -1.80 °C. However, the air temperature inside the chamber is limited at around 5.89 °C and will not decrease further. This might be due to some limitations of the design.

The cutting section at the polystyrene box for Peltier modules will have certain degree of leakage as it is clearance fit for the modules. The cold air might be escaped from the leakage and the heat flux from the heatsink of the hot side might enter the chamber as well. When the chamber is not 100% sealed and insulated, the chamber will have its limitation on the maximum temperature drop that it can achieve.

On the other side, the heatsink that attached to the cold side of the module has its constraint as well. The aluminium heatsink is usually made up of alloy material, hence the thermal conductivity of the heatsink will drop slightly and under performance as compared to the pure aluminium. For instance, the thermal conductivity for pure aluminium is 237 W/mK, whereas the aluminium alloy is around 190 W/mK. This results in the ineffective of heat transfer from the TEC to the heatsink and thus the process is slower. The actual cold side temperature at the module might be deviated from the temperature reading at the heatsink due to this reason, which means that the ceramic plate on the module might have lower temperature than -1.80 °C. However, due to the limitation of the heatsink in heat conduction, the air temperature does not drop further than 5.89 °C.

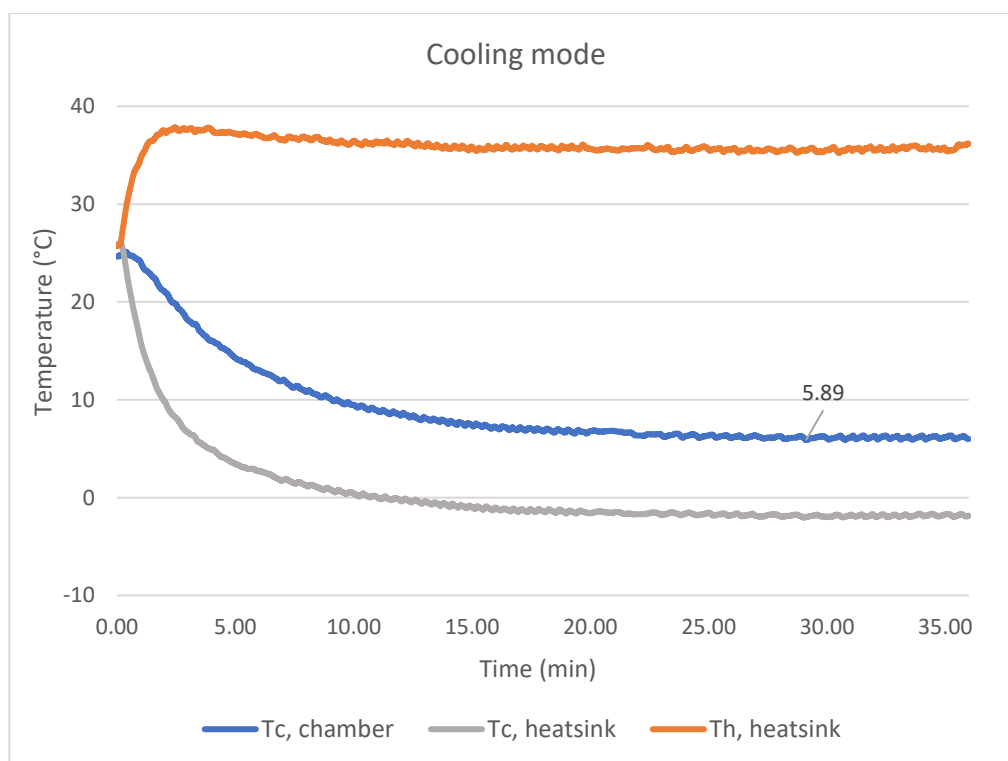


Figure 4.4: Graph of temperature profile under cooling mode

Peltier module has a characteristic of low cooling capacity. If the ceramic plate of the cold side is enclosed properly and does not expose to the ambient air, the temperature can easily go down and reach -5.34°C as shown in Table 3.2. This is because the cooling load on the module is very less as the surface is covered in a closed space. However, once the cold plate is exposed to the air, the temperature will rise up for some degree Celsius as the ambient air is a huge cooling load to the module. The cold side temperature might only reach 0°C under same current input. This is the properties of Peltier module as this small thin plate has its constraints on cooling load.

Therefore, in order to obtain low temperature at the cooling chamber, the heatsink at the cold side must be insulated from the environment and fully embedded inside of the chamber. To achieve this, the cutting area on the polystyrene box is dimensioned according to the size of heatsink, so that the heatsink can fit into the polystyrene properly with minimum leakage.

Table 4.2 shows the total amount of power consumption when the Peltier modules is running at cooling mode. As the power supply of TECs are running at constant current mode, the figure of voltage is an average value

because the voltage will be fluctuating throughout its operation. The total power needed to operate the cooling chamber is 128.86 W.

Table 4.2: Power consumption of equipment under cooling mode

	TEC 1 & 2	TEC 3 & 4	9 cm fan	4 cm fan
Voltage (V)	19.79	18.63	12.0	10.0
Current (I)	3.00	3.00	0.8	0.4
Power (W)	59.37	55.89	9.6	4.0

In overall, the performance of cooling chamber is excellent with equilibrium temperature at 5.89 °C. The chamber achieves equilibrium state within 30 minutes at ambient temperature of 25 °C.

4.3.1 Cooling load test

After the equilibrium state is achieved inside the cooling chamber, a glass of 500 ml water is placed inside the chamber to experiment the cooling power of the chamber. As shown in Figure 4.5, the water is put to the chamber at minute 30 and the test is run for 1 hour. The temperature of the water able to decrease from 26.47 °C to 15.95 °C in about 1 hour. Although it is not close to the normal chilled drink temperature at 5 °C, 15.95 °C is also a refreshing serving temperature for beverage. If the experiment is let to run for another hour, the temperature will eventually be same with the air temperature inside the chamber, as it requires more time to remove the heat from the water.

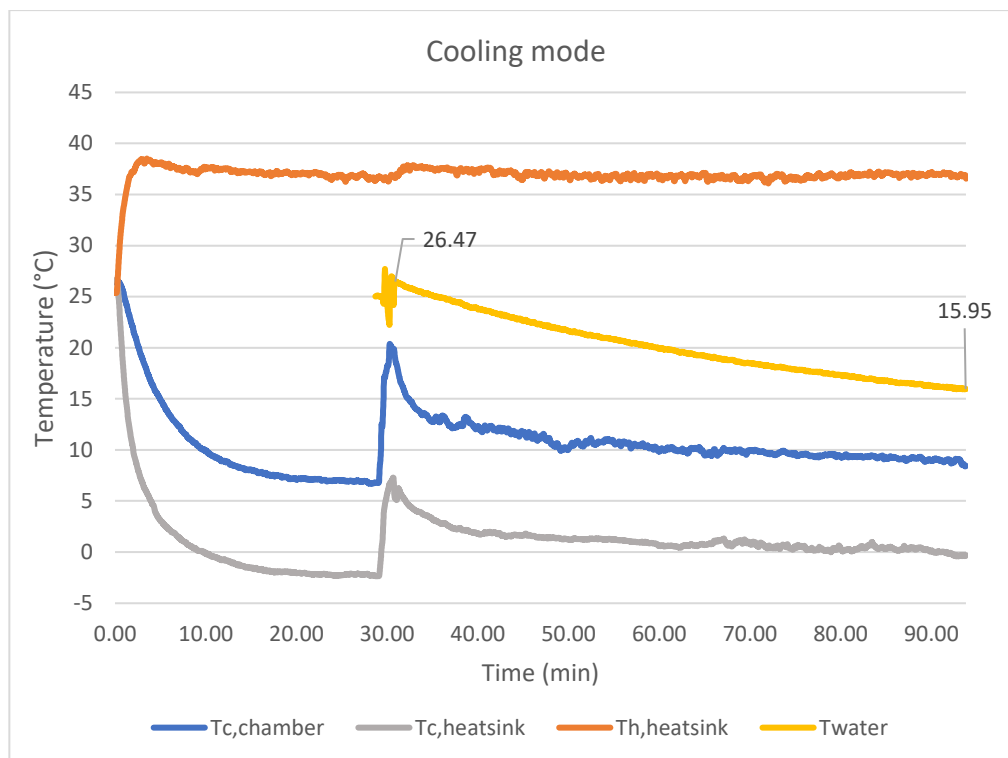


Figure 4.5: Graph of temperature profile with heat load test under cooling mode

One thing to note that is the air temperature of the chamber does not reach the same level as before the insertion of water. Before the water is placed inside the chamber, the air temperature is around 6 °C, however, the temperature increases to about 10 °C after the water is placed in the chamber. This is due to the heat load to the chamber, the thermal energy inside the water is transferred to the air, hence the temperature rises inside the chamber. However, if the test continues to run for longer time, the temperature of the chamber and water will keep decreasing. The last point of the curve shows that there is a gradient on the downward trends, although the gradient is very small of the chamber temperature.

With the temperature data, some calculations can be done to analyze the performance of the prototype in quantitative approach. The amount of heat rejected from the water can be calculated by the equation 4.1.

$$Q = mc\Delta T \quad (4.1)$$

where

Q = heat energy, J

m = mass of the substance, kg

c = specific heat capacity, J/kgK

ΔT = change in temperature, K

Calculation

$$Q = 0.5 \text{ kg} \times 4184 \frac{\text{J}}{\text{kgK}} \times (26.47 - 15.95) \text{ K}$$

$$Q = 22\,007.84 \text{ J}$$

$$\dot{Q}_C = \frac{Q}{t} = \frac{22\,007.84 \text{ J}}{3600 \text{ s}}$$

$$\dot{Q}_C = 6.11 \text{ W}$$

$$COP = \frac{\dot{Q}_C}{W}$$

$$COP = \frac{6.11 \text{ W}}{128.86 \text{ W}}$$

$$COP = 0.05$$

From the calculation, the COP of the cooling chamber is 0.05 only. The COP value is very low as it indicates that the performance of the Peltier module is not efficient. The power supplied at the Peltier modules does not successfully convert into useful cooling power at the chamber thus resulting in low COP value. The example of energy loss includes heat leakage of the chamber, Joule heating effect from the Peltier module and even from the connection wires. There are a lot of crocodile clips used during the experiment, it might be one of the sources of energy loss as the wires might get warm over long operating time. As a result, the resistance of the wire increases and the Joule heating effect also takes place. These are some of the factors that contribute to the low COP of the system.

4.3.2 Comparison with theoretical value

Based on the datasheet of the TEC1-12706 as shown in appendix, the theoretical cooling power and power consumption of the modules can be calculated. There are two categories of performance curve in the datasheet, one is for hot side temperature at 25 °C and the other one is for 50 °C. From the experiment result, the heatsink at the hot side has a temperature of about 36.0 °C, hence the performance curve at $T_h = 50$ °C is selected. Besides, at equilibrium state, the temperature difference between hot side and cold side is about 38.0 °C. Therefore, the data is referred by $DT = 40$ °C at $T_h = 50$ °C with 3.0 A current supply.

From datasheet:

Cooling power per unit, Q_c : 10 W

Power consumption per unit, P : 9.0 V x 3.0 A = 27.0 W

$$COP = \frac{4 \times 10 \text{ W}}{4 \times 27 \text{ W}}$$

$$COP = 0.37$$

The theoretical calculation of COP is much higher than the experimental value. This is because the theoretical calculation neglects the heat flux from the surroundings, heat leakage and adverse effect of Joule heating from the module itself. Therefore, the theoretical value of COP is quite excellent and much higher than the experimental value.

4.4 Heating mode

When the Peltier modules are used for heating purpose, the performance is excellent as it reaches 61.66 °C in about 25 minutes. From Figure 4.6, the curve of chamber temperature and heatsink at the hot side increase exponentially. The heatsink at the hot side records a very high temperature of 77.90 °C, while the temperature of cold side is 21.27 °C.

The primary function of the Peltier module is to absorb the heat from the cold side and reject the energy to the surrounding at the hot side. However, when the hot side of the module is enclosed in a container, the heat reservoir is

limited into the chamber only. Hence, the thermal energy is accumulating inside the chamber and could not release to the ambient. Other than the heat absorbed at the cold side, the electric current that supply to the module also results in Joule heating effect. This will lead to more amount of heat energy generated at the hot side of the module and the temperature is kept increasing. As a result, the temperature of the chamber grows exponentially because the waste heat is trapped inside of the chamber.

The temperature at the cold side is dropping for a few minutes before it starts to rise up and maintain equilibrium at around 20 °C. At the beginning of operation, the Peltier module works normally to create temperature difference between its two ceramic plates. However, when the temperature at the hot side is increasing, the cold side temperature will stop decreasing and rise up. This is because the cold side temperature fully depends on the hot side temperature; the lower temperature at hot side, the lower the cold side temperature can achieve. As the hot side temperature reaches extremely high at 77.90 °C, the cold side temperature maintains at about 21.50 °C, creating a temperature difference of 56 °C. The cooling effect on the cold side is the least at this condition, as the cold side temperature is only about 20 °C.

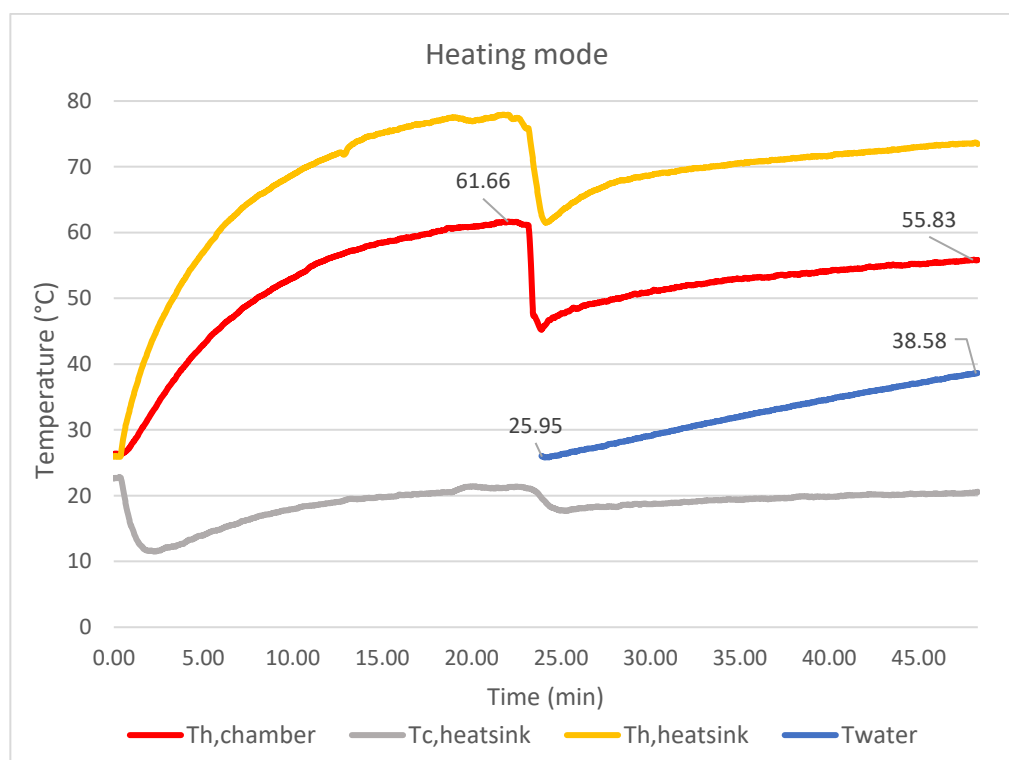


Figure 4.6: Graph of temperature profile under heating mode

Under heating mode, the Peltier modules consume more power as compared to cooling mode. As shown in Table 4.3, the total power required is 151.84 W, which is 22.98 W higher than cooling mode. This is due to the internal resistance of the Peltier module; the resistance of the module will increase when the temperature increases. Under heating mode, the temperature at the hot side is extremely hot and the cold side also becomes warmer, this results in the increase of internal resistance of the module. As a result, total power required for heating mode is much higher than cooling mode.

Table 4.3: Power consumption of equipment under heating mode

	TEC 1 & 2	TEC 3 & 4	9 cm fan	4 cm fan
Voltage (V)	23.15	22.93	12.0	10.0
Current (I)	3.00	3.00	0.8	0.4
Power (W)	69.45	68.79	9.6	4.0

In general, the performance of heating chamber is better than cooling chamber. The temperature increment in heating mode is faster and higher than the temperature decrement in cooling mode. The temperature increases for 36.66 °C in about 20 minutes from ambient temperature, whereas the temperature only decreases for 19.11 °C in 30 minutes for cooling mode. It can be concluded that the heating effect is easier to achieve by Peltier module as the Joule heating effect is added to the system.

4.4.1 Heating test

Same as cooling chamber, a sample of 500 ml water is placed inside the heating chamber once it reaches equilibrium condition. By referring to Figure 4.6, the temperature of water increases from 25.95 °C to 38.58 °C in about 25 minutes. If the experiment continues, the temperature of the water will be keep increasing as the gradient of the curve is very high. However, the experiment is completed in about 50 minutes to prevent the Peltier module from overheating. As the waste heat is trapped within the chamber, the temperature of the module is increasing and it might cause the module to burn. Therefore, the experiment is run for adequate timing only until the temperature curve is obtained.

The characteristic of the heating test also same as cooling mode, the air temperature of the chamber does not meet its original value before the insertion of water sample. This is due to the water will absorb the thermal energy of the chamber, thus decreases the air temperature of the chamber. The thermal energy from the TEC is transferred to the water by convection. Heat conduction also might occur through the wall of the water container, but the convection effect shall be more dominant. Equation 4.1 is applied to calculate the performance of heating chamber as well.

Calculation

$$Q = 0.5kg \times 4184 \frac{J}{kgK} \times (38.58 - 25.95)K$$

$$Q = 26\,421.96\,J$$

$$\dot{Q}_h = \frac{Q}{t} = \frac{26\,421.96\,J}{25 \times 60\,s}$$

$$\dot{Q}_h = 17.61\,W$$

$$COP = \frac{\dot{Q}_h}{W}$$

$$COP = \frac{17.61\,W}{151.84\,W}$$

$$COP = 0.12$$

From the calculation, the COP of the heating chamber is 0.12. The COP of heating chamber is higher than the cooling mode. This is because the Joule heating effect of the electrical current is added into the heating effect, whereas the Joule heating effect is a deficit under cooling mode. Therefore, due to both heating effect coming from Peltier and Joule effect, the COP of heating mode is much higher than the cooling mode.

4.4.2 Comparison with theoretical value

Unlike the cooling mode, the datasheet of the TEC does not have specification of heating capacity. The heat load can be calculated by the sum of cooling capacity and electrical power. This is because the heat absorbed at the cold side will be released at the hot side, plus with the Joule heating effect that added to the thermal energy at the hot side.

The temperature difference between hot and cold side of the module is about 56.03 °C under heating mode while the hot side temperature is 77.90 °C. Therefore, the data is referred at $T_h = 50$ °C with $DT = 60$ °C.

However, the cooling power Q_c could not be retrieved from the datasheet. The performance curve shows that the cooling power is 0 W when the DT is 50 °C at $T_h = 50$ °C. This explains that there is no cooling effect on the cold side of the TEC when the temperature difference is too high. Therefore, the COP of the heating mode can only be calculated as there is no cooling power on the cold side.

From datasheet:

Power consumption per unit: $10.0 \text{ V} \times 3.0 \text{ A} = 30 \text{ W}$

$$COP = \frac{Q_c + P}{P}$$

$$COP = \frac{0 + 4 \times 30}{4 \times 30}$$

$$COP = 1.0$$

As the cooling power is zero on the cold side, the heat energy that pumped out from the hot side shall be fully produced by the electrical Joule energy only. Therefore, the COP of the system is 1 which means that 100 % of electrical energy is converted to thermal energy on Peltier module. However, this is only the theoretical value for the experiment, the actual COP is 0.12 only as some of the heat energy is lost, such as lost to the ambient air or within the connection wires.

4.5 Simultaneous cooling and heating mode

After cooling and heating mode are tested separately, two chambers are attached to the cold side and hot side of the Peltier modules simultaneously to test the functionality of simultaneous cooling and heating mode. Figure 4.7 shows the result of the operation mode, the cooling chamber able to maintain at 9.66 °C and the heating chamber at 39.09 °C when both chambers reach equilibrium state. The response of the system is quite excellent as the chambers achieve equilibrium state within 20 minutes only.

As mentioned earlier, the hot chamber is opened for a gap of about 2 cm to allow some of the heat energy to release from the chamber. If the hot chamber is fully enclosed, the temperature of the cold chamber will rise up due to the increase in hot side temperature. Therefore, a certain degree of exhaust is necessary at the hot chamber so that the hot chamber can maintain at a warm temperature, while not causing the cold chamber temperature to rise up. It can be noticed that the $T_{c,heatsink}$ does not fall below 0 °C anymore as in cooling mode. This is because the $T_{h,heatsink}$ also increases to about 40 °C, which is slightly higher than in cooling mode. The TEC will maintain its temperature difference at a constant supply current hence the cold side temperature will increase along with the hot side temperature.

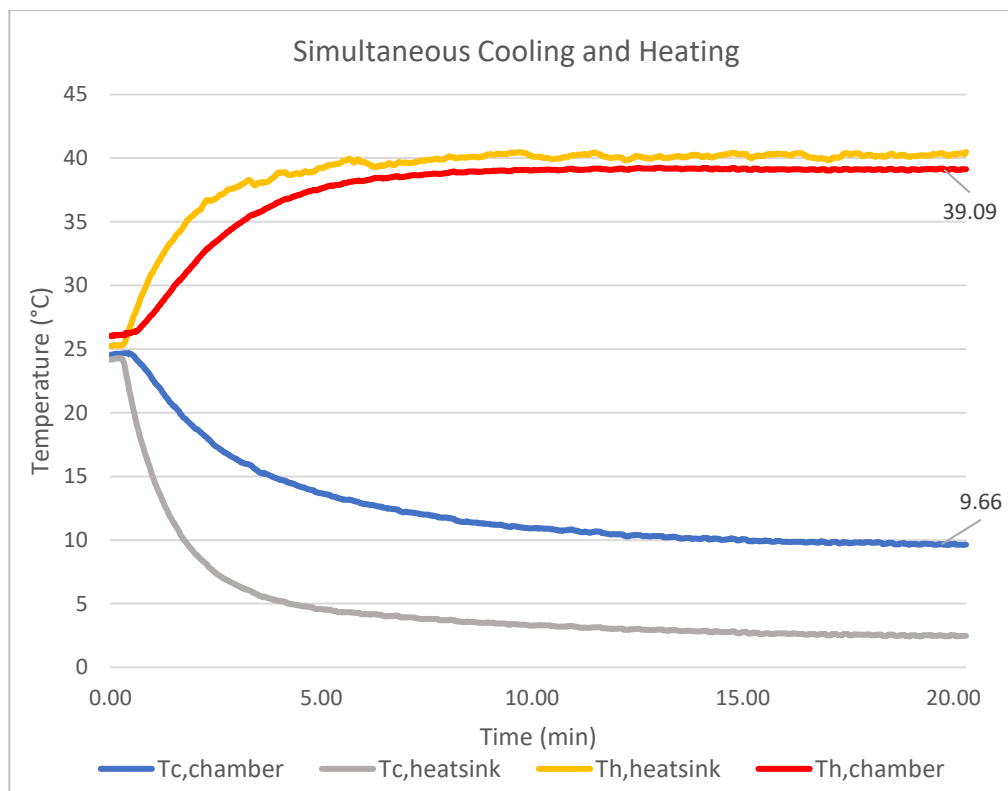


Figure 4.7: Graph of temperature profile under simultaneous cooling and heating mode

The total power consumption for this operation mode is summarized in Table 4.4. The total power required is 120.99 W, which is in between the cooling mode and heating mode. The power is slightly higher than the cooling mode as the hot side temperature of the module is increased slightly, hence the resistance of module increases as well. Meanwhile, the power required for simultaneous mode is lower than the heating mode because the temperature of the modules do not get extremely high. The internal resistance of the modules is still low and does not increase drastically, so that the power required for operation is lower than the heating mode.

Table 4.4: Power consumption of equipment under simultaneous cooling and heating mode

	TEC 1 & 2	TEC 3 & 4	9 cm fan	4 cm fan
Voltage (V)	20.46	19.87	12.0	10.0
Current (I)	3.00	3.00	0.8	0.4
Power (W)	61.38	59.61	9.6	4.0

This simultaneous operation mode provides an insight on the capabilities of thermoelectric module. The TEM is always used for specific purpose only, either for cooling, heating or generating power. When the module is only used for one purpose, the energy produced at the other side of the module is wasted. Therefore, this simultaneous operation mode utilizes the energy generated at both sides of the module and turn it into useful work.

4.5.1 Theoretical calculation on COP

The water sample heating and cooling test are not performed for this operation mode as the main interest is on the equilibrium air temperature of both chambers. However, the theoretical COP value can be calculated as well based on the performance curves of the TEC.

The temperature difference between the hot and cold side of the module is about 30 °C, while the hot side temperature is about 40 °C. The data from the datasheet is referred at $T_h = 50$ °C with $DT = 30$ °C.

From datasheet:

Cooling power per unit, $Q_c = 16.0$ W

Power consumption per unit, $P = 27.0$ W

$$COP_c = \frac{4 \times 16 \text{ W}}{4 \times 27 \text{ W}}$$

$$COP_c = 0.59$$

$$COP_h = \frac{4 \times (16 + 27) \text{ W}}{4 \times 27 \text{ W}}$$

$$COP_h = 1.59$$

By theoretical calculation, the COP of cooling chamber is 0.59 while the COP of heating chamber is 1.59. The value is the highest among the three different operation modes. This is because the temperature difference between the hot side and cold side of the module is low. The characteristic of the Peltier module is, the lower the temperature difference, the higher the cooling power. This can be explained by the phenomena where the temperature at the cold side will increase drastically whenever it is directly expose to the open air. As the cooling capacity of the module is low, the temperature at the cold side must increase as it could not cool down the huge heat load rapidly.

On the other hand, the COP for heating chamber is 1.59 which is 1.0 higher than cooling mode. This is similar to the Carnot cycle where the COP of the heat pump is always COP of the refrigeration cycle plus 1.0. However, the value is only theoretical calculation without consideration of any heat losses. It gives a good insight on the application of simultaneous cooling and heating effect so that both side energy can be utilized.

4.6 Summary

The Peltier modules TEC1-12706 have shown excellent performance whether under cooling, heating or simultaneous cooling and heating mode. The cooling chamber able to obtain lowest temperature at 5.89 °C, while the heating chamber able to obtain highest temperature at 61.66 °C when the two chambers are running separately. On the other side, the simultaneous mode able to get 9.66 °C at cooling chamber and 39.09 °C at heating chamber under equilibrium state.

Each operation mode in this study has successfully provided a good insight to develop an end-user product in the future works. For instance, the cooling mode is suitable for outdoor portable mini fridge. The size and design of the chamber are small and simple, there is no complex mechanical component such as the conventional vapour compression cycle. The beverages can be stored in the chamber to chill it during the hot scorching day. It can be powered up by the car battery as the nominal voltage output of a car battery is about 12.0 V. Moreover, the design can be cooperated into mini fridge in the hotel room also, as it is low in cost, small in size and noise-free operation.

Furthermore, the heating mode is ideal to warm up a food. As the guideline published by the U.S. Food and Drug Administration (FDA), the ideal serving temperature of the hot food is 60 °C (FDA, 2020). It can be accomplished by the hot chamber as it able to achieve 61.66 °C within 25 minutes. For instance, the cooled food during picnic can be warmed up before serving.

Last but not least, the simultaneous cooling and heating chamber can be proposed for food truck business. During the business hour, the food truck has to store their fresh foods inside the fridge throughout the day, such as vegetables, fruits and dairy products. At the same time, they might need to

defrost the frozen food from the freezer such as meats. In this context, the heating chamber at the side of cold chamber can be used to accelerate the defrosting process. The temperature is not too high until it might cook the frozen foods, it is only about 39 °C where is slightly above ambient temperature only.

In short, three operation modes for the Peltier module have successfully achieve the objective of developing a hybrid storage system. The performance of the TECs in three different modes is summarized in the Table 4.5.

Table 4.5: COP of chamber under three different operation modes

Operation mode	Experimental		Theoretical	
	COP _C	COP _H	COP _C	COP _H
Cooling	0.05		0.37	
Heating		0.12		1.0
Simultaneous			0.59	1.59

CHAPTER 5

CONCLUSIONS AND RECOMMENDATIONS

5.1 Conclusions

The objectives of this study have been successfully accomplished. A hybrid cooler and warmer storage system is built by using thermoelectric module. Two chambers are built with polystyrene box as the insulation material, the inner wall is layered with thin aluminium sheet to improve the thermal conductivity of the chamber. Besides, the fan and heatsink are attached to the thermoelectric module to increase the heat convection effect.

Before the actual prototyping process, a computational fluid dynamic (CFD) simulation model is developed to proof the design concept. ANSYS software is used in this study, with the analysis system of Fluid Flow (Fluent). The internal fluid volume of the chamber is sketched out and the temperature data of the Peltier module is used as the input for the model. From the result, it proves that four units of Peltier modules can provide a satisfactory of cooling power to the chamber. Therefore, four units of single stage Peltier modules are implemented in the prototype.

There are total of three operation modes in this design, which are cooling mode, heating mode, and simultaneous cooling and heating mode. Under cooling the mode, the chamber temperature able to achieve 5.89 °C and reach equilibrium state within 30 minutes. Next, the chamber temperature able to achieve 61.66 °C within 20 minutes when it is run under heating mode. Lastly, under simultaneous cooling and heating mode, the cooling chamber can achieve 9.66 °C while the heating chamber at 39.09 °C, the chambers reach equilibrium within 20 minutes.

The experimental COP of the chamber is below 0.2 on both cooling and heating modes. This might be due to the heat leakage from the insulation chamber, Joule heating effect on the connection wires and even constraint of the heatsink. Theoretical calculation shows that the simultaneous mode has the highest COP among three different modes. This is because the temperature

difference at simultaneous mode is lower, thus increasing the cooling capacity and heating capacity of the thermoelectric module.

In conclusion, the hybrid storage system has been constructed successfully and its performance is quite promising for developing the finished products to the market. Its applications include mini fridge, food warmer and defrosting chamber. The advantages of small in size, simple design and low cost make the interest of this prototype to be implemented in the real-life applications. In short, thermoelectric module has a remarkable performance in both cooling and heating effect with small size and simple design.

5.2 Recommendations for future work

In future works, the prototype can be powered up by solar cells. The nominal voltage for the thermoelectric module is about 10 V and 3.0 A. This is sufficient to be supplied by the solar cells so that the product does not rely on the electrical power supply. For instance, portable mini fridge during picnic might not have power supply or even car battery to power up the product. Therefore, solar power is an alternative approach to charge up the thermoelectric module and the fan.

In addition, the solar cells can be cooperated with the thermoelectric generator, which the Peltier module is used to generate electricity for the Peltier module that use for cooling. This is named as the self-driven TEG-TEC system as mentioned in the Chapter 2.6. This would develop a self-sustainable device that can operate without external power supply. Although the initial cost will be high, it can save a lot of money if it is used for long term period.

REFERENCES

- Abdul-Wahab, S.A., Elkamel, A., Al-Damkhi, A.M., Al-Habsi, I.A., Al-Rubai'ey', H.S., Al-Battashi, A.K., Al-Tamimi, A.R., Al-Mamari, K.H. and Chutani, M.U., 2009. Design and experimental investigation of portable solar thermoelectric refrigerator. *Renewable Energy*, 34(1).
- AFSHARİ, F., 2020. Experimental Study for Comparing Heating and Cooling Performance of Thermoelectric Peltier. *Journal of Polytechnic*, 0900(3), pp.889–894.
- Aliabadi, P., Mahmoud, S. and AL_Dadah, R.K., 2014. Simulation of Cascaded Thermoelectric Devices for Cryogenic Medical Treatment. (Equation 2), pp.1–4.
- Belovski, I.R. and Aleksandrov, A.T., 2019. Examination of the Characteristics of a Thermoelectric Cooler in Cascade. *10th National Conference with International Participation, ELECTRONICA 2019 - Proceedings*, pp.1–4.
- Çağlar, A., 2018. Optimization of operational conditions for a thermoelectric refrigerator and its performance analysis at optimum conditions. *International Journal of Refrigeration*, 96, pp.70–77.
- Cai, Y., Wang, Y., Liu, D. and Zhao, F.Y., 2019. Thermoelectric cooling technology applied in the field of electronic devices: Updated review on the parametric investigations and model developments. *Applied Thermal Engineering*, [online] 148(September 2018), pp.238–255. Available at: <<https://doi.org/10.1016/j.applthermaleng.2018.11.014>>.
- Dai, Y.J., Wang, R.Z. and Ni, L., 2003. *Experimental investigation and analysis on a thermoelectric refrigerator driven by solar cells. Solar Energy Materials and Solar Cells*, .
- FDA, 2020. *Serving Up Safe Buffets*. [online] Available at: <<https://www.fda.gov/food/buy-store-serve-safe-food/serving-safe-buffets#:~:text=Take%20Temperatures>>.
- Gao, Y.W., Lv, H., Wang, X.D. and Yan, W.M., 2017. Enhanced Peltier cooling of two-stage thermoelectric cooler via pulse currents. *International Journal of Heat and Mass Transfer*, [online] 114, pp.656–663. Available at: <<http://dx.doi.org/10.1016/j.ijheatmasstransfer.2017.06.102>>.
- He, W., Zhang, G., Zhang, X., Ji, J., Li, G. and Zhao, X., 2015. Recent development and application of thermoelectric generator and cooler. *Applied Energy*, [online] 143, pp.1–25. Available at: <<http://dx.doi.org/10.1016/j.apenergy.2014.12.075>>.
- He, W., Zhou, J., Hou, J., Chen, C. and Ji, J., 2013. Theoretical and

experimental investigation on a thermoelectric cooling and heating system driven by solar. *Applied Energy*, [online] 107, pp.89–97. Available at: <<http://dx.doi.org/10.1016/j.apenergy.2013.01.055>>.

Hermes, C.J.L. and Barbosa, J.R., 2012. Thermodynamic comparison of Peltier, Stirling, and vapor compression portable coolers. *Applied Energy*, 91(1), pp.51–58.

Ibañez-Puy, M., Bermejo-Busto, J., Martín-Gómez, C., Vidaurre-Arbizu, M. and Sacristán-Fernández, J.A., 2017. Thermoelectric cooling heating unit performance under real conditions. *Applied Energy*, 200, pp.303–314.

Jugsujinda, S., Vora-Ud, A. and Seetawan, T., 2011. Analyzing of thermoelectric refrigerator performance. *Procedia Engineering*, [online] 8, pp.154–159. Available at: <<http://dx.doi.org/10.1016/j.proeng.2011.03.028>>.

Kamasi, D.D., Zainulloh, M., Nadhir, A. and Sakti, S.P., 2020. Comparison between two-stage and three-stage Peltier thermoelectric coolers driven by pulse width modulation. *Journal of Physics: Conference Series*, 1528.

Karimi, G., Culham, J.R. and Kazerouni, V., 2011. Performance analysis of multi-stage thermoelectric coolers. *International Journal of Refrigeration*, [online] 34(8), pp.2129–2135. Available at: <<http://dx.doi.org/10.1016/j.ijrefrig.2011.05.015>>.

Karwa, N., Stanley, C., Intwala, H. and Rosengarten, G., 2017. Development of a low thermal resistance water jet cooled heat sink for thermoelectric refrigerators. *Applied Thermal Engineering*, [online] 111, pp.1596–1602. Available at: <<http://dx.doi.org/10.1016/j.applthermaleng.2016.06.118>>.

Li, W.K., Chang, J.H., Amani, M., Yang, T.F. and Yan, W.M., 2019. Experimental study on transient supercooling of two-stage thermoelectric cooler. *Case Studies in Thermal Engineering*, 14(May).

Lin, L., Zhang, Y.F., Liu, H.B., Meng, J.H., Chen, W.H. and Wang, X.D., 2019. A new configuration design of thermoelectric cooler driven by thermoelectric generator. *Applied Thermal Engineering*, [online] 160(April), p.114087. Available at: <<https://doi.org/10.1016/j.applthermaleng.2019.114087>>.

Ma, M. and Yu, J., 2014. An analysis on a two-stage cascade thermoelectric cooler for electronics cooling applications. *International Journal of Refrigeration*, 38(1).

Meng, F., Zhang, L., Li, J., Li, C., Xie, L., Luo, Y. and Liu, Z., 2015. Investigation of Thermoelectric Warm Air Heater. *Energy Procedia*, 75, pp.621–626.

Meng, J.H., Wang, X.D. and Zhang, X.X., 2013. Transient modeling and dynamic characteristics of thermoelectric cooler. *Applied Energy*, [online] 108,

pp.340–348. Available at: <<http://dx.doi.org/10.1016/j.apenergy.2013.03.051>>.

Nami, H., Nemati, A., Yari, M. and Ranjbar, F., 2017. A comprehensive thermodynamic and exergoeconomic comparison between single- and two-stage thermoelectric cooler and heater. *Applied Thermal Engineering*, [online] 124, pp.756–766. Available at: <<http://dx.doi.org/10.1016/j.applthermaleng.2017.06.100>>.

Parashchuk, T., Sidorenko, N., Ivantsov, L., Sorokin, A., Maksymuk, M., Dzungza, B. and Dashevsky, Z., 2021. Development of a solid-state multi-stage thermoelectric cooler. *Journal of Power Sources*, [online] 496(March), p.229821. Available at: <<https://doi.org/10.1016/j.jpowsour.2021.229821>>.

Provensi, A. and Barbosa, J.R., 2020. Analysis and optimization of air coolers using multiple-stage thermoelectric modules arranged in counter-current flow. *International Journal of Refrigeration*, 110, pp.19–27.

Rahman, S.M.A., Hachicha, A.A., Ghenai, C., Saidur, R. and Said, Z., 2020. Performance and life cycle analysis of a novel portable solar thermoelectric refrigerator. *Case Studies in Thermal Engineering*, 19(January), pp.1–16.

Saidur, R., Masjuki, H.H., Hasanuzzaman, M., Mahlia, T.M.I., Tan, C.Y., Ooi, J.K. and Yoon, P.H., 2008. Performance investigation of a solar powered thermoelectric refrigerator. *International Journal of Mechanical and Materials Engineering*, 3(1), pp.7–16.

Sastri, V.R., 2010. *Chapter 6 - Commodity Thermoplastics: Polyvinyl Chloride, Polyolefins, and Polystyrene*. [online] ScienceDirect. Available at: <<https://www.sciencedirect.com/science/article/pii/B9780815520276100066>>.

Sm, S., Prof, A., Gnanasekaran, K., Prof, A., Johnson, S., Prof, S.A. and Samuel, J., 2018. Performance study on thermoelectric cooling and heating system with cascaded and integrated approach. ~ 1348 ~ *International Journal of Chemical Studies*, [online] 6(1), pp.1348–1354. Available at: <<https://www.chemijournal.com/archives/?year=2018&vol=6&issue=1&ArticleId=1777&si=false>>.

Sulaiman, A.C., Amin, N.A.M., Basha, M.H., Majid, M.S.A., Nasir, N.F.B.M. and Zaman, I., 2018. Cooling Performance of Thermoelectric Cooling (TEC) and Applications: A review. *MATEC Web of Conferences*, 225, pp.1–10.

Tian, M.W., Aldawi, F., Anqi, A.E., Moria, H., Dizaji, H.S. and Wae-hayee, M., 2021. Cost-effective and performance analysis of thermoelectricity as a building cooling system; experimental case study based on a single TEC-12706 commercial module. *Case Studies in Thermal Engineering*, [online] 27(March), p.101366. Available at: <<https://doi.org/10.1016/j.csite.2021.101366>>.

Yilmazoglu, M.Z., 2016. Experimental and numerical investigation of a prototype thermoelectric heating and cooling unit. *Energy and Buildings*, 113.

Zhao, D. and Tan, G., 2014. A review of thermoelectric cooling: Materials, modeling and applications. *Applied Thermal Engineering*, [online] 66(1–2), pp.15–24. Available at: <<http://dx.doi.org/10.1016/j.applthermaleng.2014.01.074>>.

APPENDICES

Appendix A: Figures

Item Code	Rated Voltage	Rated Current (A)	Input Power (W)	Speed RPM	Max. Air Flow		Noise dB(A)
					CFM	m ³ /min	
AD05V40-10T-FPH-B7-N1	5V	0.18	0.9	7000	6.3	0.18	31
AD05V40-10T-FPH-B7-N2	5V	0.14	0.7	6000	5.4	0.15	26
AD12V40-10T-FPH-B7-N1	12V	0.10	1.2	7000	6.3	0.18	31
AD12V40-10T-FPH-B7-N2	12V	0.09	1.1	6000	5.4	0.15	26
AD24V40-10T-FPH-B7-N1	24V	0.06	1.4	7000	6.3	0.18	31

Figure A-1: Datasheets of the 4 cm Computer Fan

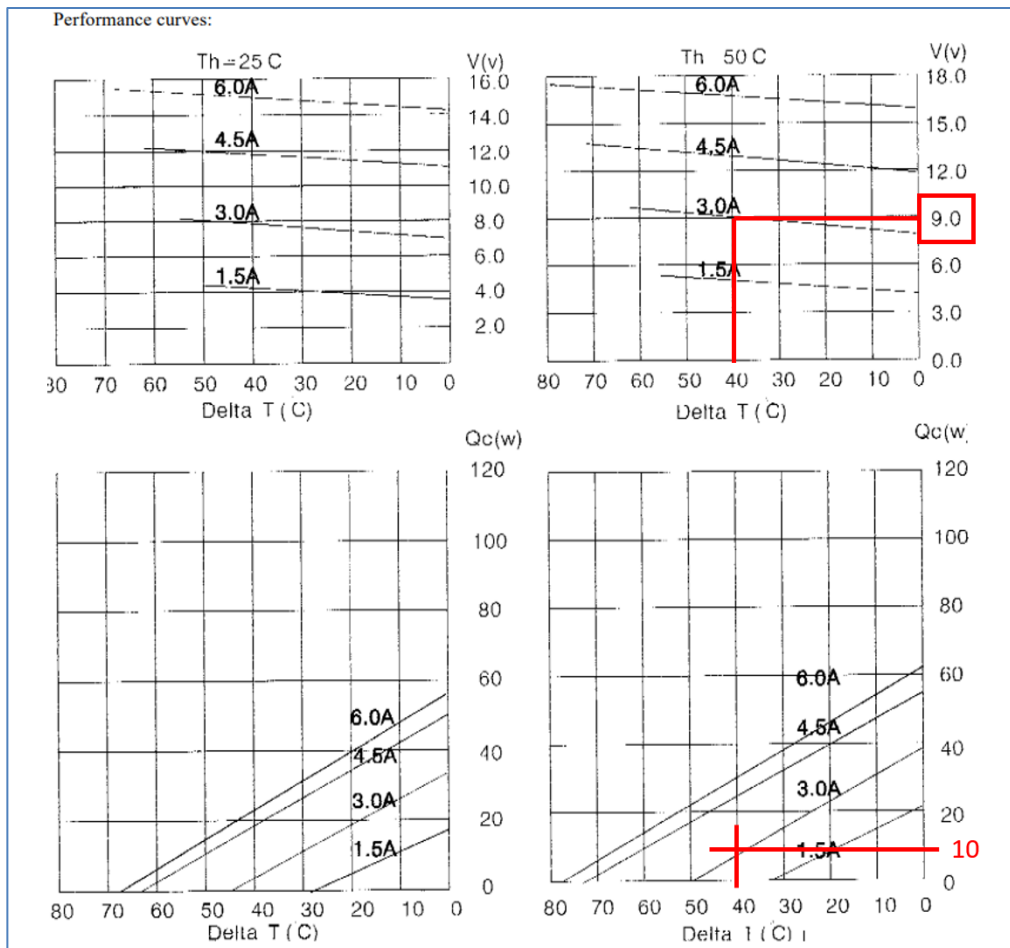


Figure A-2: Performance curves of TEC1-12706

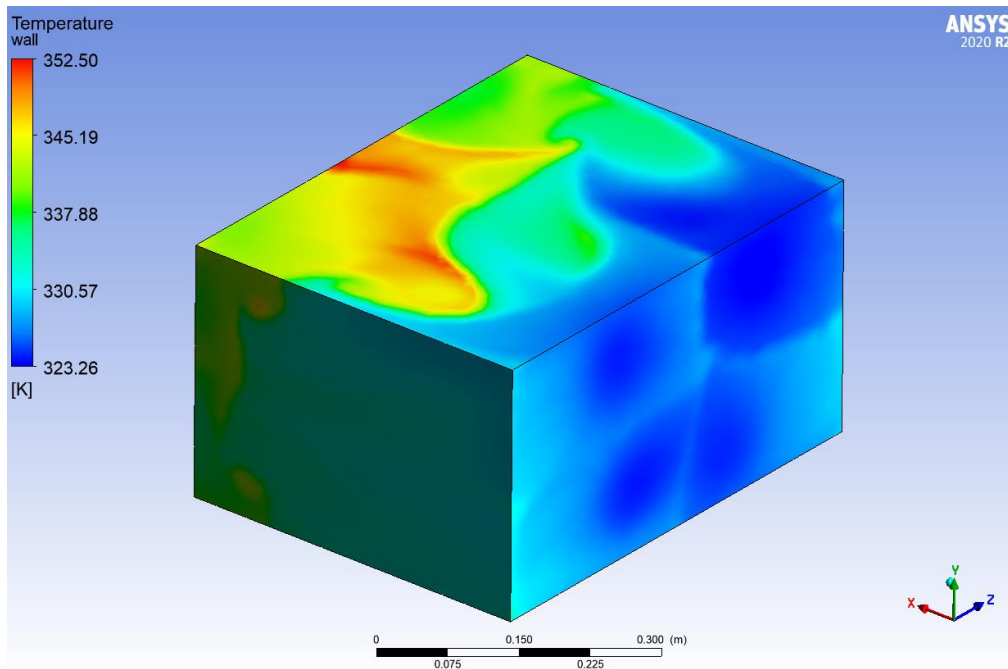


Figure A-3: Temperature distribution on wall with 300K inlet air



APPLIED ENERGY

Thermodynamic comparison of Peltier, Stirling, and vapor compression portable coolers

Author: Christian J.L. Hermes, Jader R. Barbosa

Publication: Applied Energy

Publisher: Elsevier

Date: March 2012

Copyright © 2011 Elsevier Ltd. All rights reserved.

Journal Author Rights

Please note that, as the author of this Elsevier article, you retain the right to include it in a thesis or dissertation, provided it is not published commercially. Permission is not required, but please ensure that you reference the journal as the original source. For more information on this and on your other retained rights, please visit: <https://www.elsevier.com/about/our-business/policies/copyright#Author-rights>

BACK
CLOSE WINDOW

Figure A-4: Rights of Figure 2.1



A comprehensive thermodynamic and exergoeconomic comparison between single- and two-stage thermoelectric cooler and heater

Author: Hossein Nami, Arash Nemat, Mortaza Yari, Faramarz Ranjbar

Publication: Applied Thermal Engineering

Publisher: Elsevier

Date: September 2017

© 2017 Elsevier Ltd. All rights reserved.

Journal Author Rights

Please note that, as the author of this Elsevier article, you retain the right to include it in a thesis or dissertation, provided it is not published commercially. Permission is not required, but please ensure that you reference the journal as the original source. For more information on this and on your other retained rights, please visit: <https://www.elsevier.com/about/our-business/policies/copyright#Author-rights>

[BACK](#) [CLOSE WINDOW](#)

Figure A-5: Right of Figure 2.2